# VNIR and MIR spectroscopy of PLFA-derived soil microbial properties and associated soil physicochemical characteristics in an experimental plant diversity gradient

Christopher Hutengs [a,b,c,*], Nico Eisenhauer [b,d], Martin Schädler [b,e], Alfred Lochner [b,d], Michael Seidel [a,c], Michael Vohland [a,b,c]

[a] Geoinformatics and Remote Sensing, Institute for Geography, Leipzig University, Johannisallee 19a, 04103, Leipzig, Germany

[b] German Centre for Integrative Biodiversity Research (iDiv) Halle-Jena-Leipzig, Puschstrasse 4, 04103, Leipzig, Germany

[c] Remote Sensing Centre for Earth System Research, Leipzig University, Talstr. 35, 04103, Leipzig, Germany

[d] Leipzig University, Puschstrasse 4, 04103, Leipzig, Germany

[e] Department Community Ecology, Helmholtz-Centre for Environmental Research - UFZ, Theodor-Lieser-Str. 4, 06120, Halle, Germany

[*] Corresponding author. Geoinformatics and Remote Sensing, Institute for Geography, Leipzig University, Johannisallee 19a, 04103, Leipzig, Germany.

*Keywords:*

Proximal soil sensing, Soil spectroscopy, Portable instruments, Microbial biomarkers, Plant-soil interactions, Bacterial and fungal biomass

## Abstract

Improving our understanding of the functions and processes of soil microbial communities and their interactions with the physicochemical soil environment requires large amounts of timely and cost-efficient soil data, which is difficult to obtain with routine laboratory-analytical methods. Soil spectroscopy with portable visible-to-near infrared (VNIR) and mid-infrared (MIR) instruments can fill this gap by facilitating the rapid acquisition of biotic and abiotic soil information.

In this study, we evaluated the capabilities of VNIR and MIR spectroscopy to analyze soil physicochemical and microbial properties in a long-term grassland biodiversity-ecosystem functioning experiment. Soil samples were collected at the Jena Experiment (Jena, Germany) and measured with portable VNIR and MIR spectrometers in field-moist condition to determine their potential for on-site data collection and analysis. Reference data to calibrate spectroscopic models were acquired with routine analytical methods, including PLFA extractions of microbial biomarkers. We further collected reference VNIR and MIR data on pre-treated soils (dried and finely ground) to assess the anticipated impact of field measurements on spectroscopic calibrations.

MIR spectra allowed more accurate estimates of soil physicochemical and microbial properties than VNIR data on pre-treated samples. For soils in field condition, MIR calibrations were more accurate for physicochemical properties, but VNIR data gave significantly better estimates of microbial properties. Combined VNIR/MIR estimates achieved the most accurate estimation results for all soil properties in each case.

Soil physicochemical properties could be estimated from VNIR/MIR data with high accuracy ($R^2$ = 0.72–0.99) on pre-treated soil samples, whereas the results for soil microbial properties were more moderate ($R^2$ = 0.66–0.72). On field-moist soils, estimation accuracies decreased notably for organic and inorganic carbon (ΔRMSE = 52–72%), improved slightly for soil texture (ΔRMSE = 4–7%) and decreased slightly for microbial properties (ΔRMSE = 4–9%). The VNIR/MIR estimates derived from soils in field condition were sufficiently accurate to detect experimental plant treatment effects on organic carbon, as well as bacterial and fungal biomass. We further found that spectroscopic estimates of soil microbial properties were primarily enabled through indirect correlations with spectrally active soil constituents, i.e., associations between soil microbial properties and the physicochemical soil environment.

Our findings highlight the capacity of VNIR and MIR spectroscopy to analyze the physicochemical soil environment, including potential on-site data collection and analysis on soils in field condition, and

indicate that VNIR/MIR data can estimate soil microbial properties when soil physicochemical properties shape the distribution of soil microbial communities.

## 1 Introduction

Soil microorganisms play a crucial role in the maintenance of soil ecosystem functioning, health and fertility through the decomposition of plant material, the biogeochemical cycling of nutrients, and the stabilization of soil aggregates (Chaparro et al., 2012; Bardgett and van der Putten, 2014; Fierer, 2017). The soil microbiome, in turn, is influenced by above- and belowground inputs linked to the composition of plant communities (Lange et al., 2015; Dassen et al., 2017) and the abiotic soil environment, characterized by various soil physicochemical properties, including soil pH, organic carbon quality and quantity, soil moisture, nitrogen and phosphorus, and soil texture and structure (Fierer, 2017; Xia et al., 2020). At larger spatial scales, soil microbial diversity and abundance is primarily driven by environmental factors such as climate, topography and land cover (Xue et al., 2018). Accordingly, soil microbial properties can exhibit spatial variation at multiple nested scales (Ettema and Wardle, 2002), with microbial community structure exhibiting as much variation within a single local soil sample as there is between different biomes thousands of kilometres apart (Eilers et al., 2012; Ramirez et al., 2014). Analyzing this variation may prove essential in further understanding soil microbial-plant interactions (Classen et al., 2015) , larger-scale biogeographic patterns of microbial diversity (Xue et al., 2018; Yang et al., 2019) or the response of soil microbial communities to climate change (Jansson and Hofmockel, 2020).

Efficient soil policy and management require detailed information on the distribution and diversity of soil microbial properties; however, such data is often not available at appropriate spatial and temporal scales (Guerra et al., 2020; Guerra et al., 2021). Current routine laboratory approaches (e.g., wet chemical analyses, fatty acid profiling) may be too laborious or costly to obtain physicochemical and microbial soil data at the necessary or desired spatial and temporal sampling density for such analyses (McBratney et al., 2006; Viscarra Rossel et al., 2011). Soil diffuse reflectance spectroscopy in the visible/near-infrared (VNIR) and mid-infrared (MIR) can complement routine analytical methods by providing a faster and cheaper alternative method for collecting quantitative soil data (Nocita et al., 2015; Seybold et al., 2019). Diffuse reflectance spectroscopy is sensitive to the presence and abundance of organic and inorganic molecule bonds in the near- and mid-infrared and electronic transitions in the visible electromagnetic range (Hunt, 1977; Nguyen et al., 1991). Through the interactions of electromagnetic

radiation with the soil matrix, the diffuse reflectance spectrum provides extensive information on the chemical composition of the soil (Parikh et al., 2014). The quantitative determination of soil properties with VNIR and MIR spectroscopy requires chemometric calibrations, usually with partial least squares regression (PLSR), to link the measured reflectance signal with the soil property of interest (Stenberg et al., 2010). Soil properties at additional sampling locations within the calibration domain can then be estimated from VNIR/MIR reflectance measurements without further conventional analyses.

Soil physicochemical properties (e.g., organic carbon (OC), nitrogen (N), soil carbonates (inorganic carbon, IC), clay minerals and sand (quartz) content) can generally be estimated with high accuracy as they are directly linked to several relevant absorption bands in the VNIR and MIR regions (Viscarra Rossel et al., 2006; Kuang et al., 2012; Soriano-Disla et al., 2014). In contrast, VNIR/MIR calibrations of soil microbial and biological properties have been discussed more controversially (Soriano-Disla et al., 2014; Ludwig et al., 2015). As microbial biomass in mineral soils represents only about ~5% of total soil organic matter, it seems unlikely to observe a directly related spectral signal or pattern in the VNIR or MIR (Soriano-Disla et al., 2014). Some studies, although significantly fewer than for soil physicochemical properties, have nevertheless shown that (micro)biological soil properties can be estimated spectroscopically with moderate to high accuracy (Soriano-Disla et al., 2014; Ludwig et al., 2015). These include microbial biomasses derived from PLFAs (Rinnan and Rinnan, 2007; Zornoza et al., 2008), the fungal biomarker ergosterol and microbial soil carbon (Terhoeven-Urselmans et al., 2008; Heinze et al., 2013; Vohland et al., 2017), and soil microbial biomass from 16S rRNA gene quantification (Rasche et al., 2013). VNIR/MIR estimation models have been hypothesized to rely predominantly on indirect correlations between soil biological and physicochemical properties that can be captured through a direct spectral response of, e.g., total organic matter or soil texture parameters (Zornoza et al., 2008; Ludwig et al., 2015). In this context, recently published studies have shown that much of the variation in soil bacterial abundance and diversity at different scales can be modelled by VNIR and MIR soil reflectance through its capability to characterize the soil habitat in its overall mineral and organic composition (Yang et al., 2019; Ricketts et al., 2020).

Against this background, the recent introduction of portable, high-performance MIR spectrometers (Forrester et al., 2015; Soriano-Disla et al., 2017; Hutengs et al., 2018), in conjunction with established portable VNIR instruments (Stevens et al., 2006; Kusumo et al., 2008; Terhoeven-Urselmans et al., 2008; Kuang and Mouazen, 2011), opens the opportunity for fast and cost-effective VNIR/MIR analysis of soil physicochemical and microbial properties at the local scale, e.g., in the framework of globally distributed ecological experiments or soil monitoring. First field studies with MIR measurements on

field-moist, untreated soil samples have confirmed the potential for on-site analyses of soil OC (Hutengs et al., 2019) and particle size distribution (Janik et al., 2020), with handheld MIR instruments potentially allowing more accurate OC estimates than VNIR instruments (Hutengs et al., 2019). The application of portable MIR instruments to evaluate more soil physicochemical and microbial properties, alone or together with VNIR instruments, thus merits further investigation.

In this study, we examined the potential of VNIR/MIR reflectance spectroscopy with portable instruments to analyze soil microbial properties coupled with soil physicochemical characteristics in the framework of a long-term grassland biodiversity-ecosystem functioning (BEF) experiment. We aimed to address two key issues as a fundamental prerequisite for the possible integration of VNIR/MIR analyses with portable instruments in soil microbiological and ecological research, including (i) the capability of VNIR/MIR calibrations to estimate PLFA-derived soil microbial properties and soil physicochemical characteristics in field-moist condition; (ii) whether recently introduced handheld MIR instruments bring an additional benefit for the analyses of the aforementioned soil properties, compared to VNIR instruments alone. In addition, we explored the predictive mechanisms that underlie VNIR/MIR models of soil microbial properties – indirect, i.e., mediated by spectrally active soil constituents such as OC and soil texture, vs. signals directly linked to soil microbial biomass – as these have important implications for VNIR/MIR model robustness and the ability to generalize across soil types and environmental conditions. Moreover, we aimed to explore if VNIR/MIR reflectance spectroscopy is sufficiently sensitive to detect local plant diversity and community effects on soil microbial properties.

# 2 Material and methods

## 2.1 Study site and soil sampling

Soil samples were collected at the Jena Experiment (Fig. 1; Roscher et al., 2004; Weisser et al., 2017) field site, located on the floodplain of the Saale river in Jena, Germany (50°55′N, 11°35′E), in late August 2017. The biodiversity-ecosystem functioning experiment has 80 main plots with plant communities of varying species richness (1, 2, 4, 8, 16, 60) and functional group composition (1–4 of grasses, small herbs, tall herbs or legumes) arranged in a randomized block design to account for variation in soil properties across the site (Roscher et al., 2004). The site's main soil type is a Calcaric/Eutric Fluvisol (FAO) developed from loamy fluvial deposits. The site's physicochemical soil environment is characterized by strong soil texture and soil carbonate gradients perpendicular to the Saale river. Sand content decreases strongly from ~50% in Block 1, adjacent to the river, to ~5% in Block 4 at the opposite

end of the site, while clay and soil carbonate contents increase in that direction. Block 4 also has a relatively high carbonate content (~300 g CaCO3/kg) compared to the other blocks.

**< insert Figure 1 about here >**

Topsoil samples (0–15 cm) were collected from the 80 main plots by taking cores from two adjacent subplots (160 in total) with a soil corer (~2 cm diameter; 5 cores per subplot). The subplots were originally designated to a long-term summer drought treatment (Vogel et al., 2013) that ended in 2016. A preliminary analysis showed that differences between the subplot treatments for all analyzed soil properties were marginal. We thus decided to pool the adjacent samples, which resulted in a set of 80 soil samples corresponding to the main plots of the experiment.

The collected soil samples were sieved (<2 mm), packed in plastic bags and cooled at ~4 °C until transport to the lab. Two subsamples of the material were taken for further analysis after homogenizing the soil: The first subsample was used to collect VNIR and MIR reflectance spectra on field-moist soil and was subsequently oven-dried and finely ground for routine analysis of soil physicochemical properties and to collect a second set of VNIR/MIR data on pre-treated soil material. The second subsample of the material was frozen and stored at −20 °C for PLFA analysis to derive soil microbial properties from PLFA biomarkers.

## 2.2 Laboratory analytical methods

Soil physicochemical properties were determined on oven-dried (~40 °C) and, if necessary, finely ground (<10 µm; Retsch PM 200, Retsch GmbH, Haan, Germany) soil subsamples, respectively. We determined soil moisture content ($H_2O$) as the weight difference between field-moist and oven-dried soil. Soil pH was measured in $CaCl_2$ (potential acidity) with a glass electrode according to DIN ISO 10390 (2005). Total carbon (TC) and nitrogen (N) were determined through gas chromatography after dry combustion with an elemental analyzer (Vario EL, Elementar Analysensysteme GmbH, Hanau, Germany). We measured carbonate content ($CaCO_3$) volumetrically following DIN ISO 10693 (2014). The inorganic carbon (IC) present in $CaCO_3$ was then subtracted from TC to derive soil organic carbon (OC). Soil texture information, i.e., sand and clay content, was taken from an existing plot-level database (Kreutziger et al., 2018).

We used phospholipid fatty acid (PLFA) biomarkers to characterize soil microbial properties. PLFA extraction and methylation were carried out following the protocol of Frostegård et al. (1991) as described in Wagner et al. (2015). PLFAs were analyzed with a PerkinElmer Clarus 680 gas

chromatograph, equipped with an SP-2560 capillary column (length: 100 m, diameter: 0.25 mm, film thickness: 0.2 µm) and a flame ionization detector using helium as carrier gas. PLFA biomarkers were assigned to microbial biomass groups based on Willers et al. (2015): Bacterial biomass ($PLFA_{BAC}$) was characterized by (i) gram-positive bacteria ($PLFA_{G+}$; i14:0, i15:0, a15:0, i16:0, i17:0, i18:0), (ii) gram-negative bacteria ($PLFA_{G-}$; cy17:0, cy19:0) and (iii) PLFAs widespread in bacteria (16:1ω7). The PLFAs 18:2ω6,9 (saprophytic fungi, iv) represented fungal biomass ($PLFA_{FUN}$). PLFA biomarkers (i–iv) were aggregated to determine total microbial biomass ($PLFA_{MIC}$). In addition, we considered the total abundance of PLFAs in the sample ($PLFA_{TOT}$) for analysis. We further calculated the fungal-to-bacterial PLFA biomass ratio (F:B) and the gram-positive-to-gram-negative bacterial biomass ratio (G+:G−) as composite indicators of soil microbial community structure as well as the ratio of microbial PLFA biomass ($PLFA_{MIC}$) to OC (MIC:OC).

### 2.3 VNIR and MIR spectral data measurements

Soils spectra on samples in field-moist condition were collected in the laboratory with portable VNIR (ASD FieldSpec 4) and MIR (Agilent 4300) spectrometers as these instruments potentially allow the rapid acquisition of spectral data on-site without further sample pre-treatment, either by extracting a small amount of soil or by collecting measurements directly on a clean surface free from plant residues (Hutengs et al., 2019). We additionally measured reference soil reflectance spectra on homogenized dried and finely ground samples (~10 µm) to put the results achieved with field-moist samples into context and enable a comparison with the existing literature, which primarily refers to pre-treated soils, especially in the MIR.

VNIR spectra (400–2500 nm) on pre-treated (dried and finely ground) sample material were recorded using a FOSS XDS Rapid Content Analyzer (FOSS NIRSystems Inc., Laurel, USA) with ~10 g of soil spread out evenly in a quartz-glass petri dish. The FOSS XDS is the reference instrument for the EU-wide LUCAS topsoil database and its accompanying VNIR spectral library (Origiazzi et al., 2018; Stevens et al., 2013) and allows slightly better spectral measurements and calibrations for laboratory applications on pre-treated samples than the ASD Field Spec 4 (Gholizadeh et al., 2021). For each soil sample, we measured diffuse reflectance with the FOSS XDS on two replicates at 2 nm spectral resolution with a 0.5 nm sampling interval and 32 co-added scans. Replicate spectra were then averaged into a single VNIR spectrum. The instrument was re-calibrated with an internal reflectance standard every ~30 min.

On field-moist soil samples, VNIR measurements were recorded with a portable ASD FieldSpec 4 spectroradiometer (Malvern Panalytical Inc., Almelo, The Netherlands) equipped with a contact probe attachment (Fig. 2). The loose soil (~20 g) was spread out evenly in a petri dish with a 7 cm diameter and measured in direct contact between the material surface and the probe. The contact probe included an internal halogen light source to ensure consistent illumination and measured bi-directional reflectance at a 30° viewing zenith angle over a ~3 $cm^2$ area. We measured four replicates with 32 co-added scans on each sample by rotating the contact probe by 90° after each scan to compensate for directional reflectance effects. Reflectance spectra were collected at 3 nm (400–1000 nm) and 30 nm (1000–2500 nm) spectral resolution at a sampling interval of 1 nm; a Zenith Polymer® panel was used for instrument calibration at ~10 min intervals.

**< insert Figure 2 about here >**

MIR measurements on both field-moist and pre-treated sample material were collected in a small sample holder (Fig. 2) with an Agilent 4300 Handheld FTIR (Agilent Technologies, Santa Clara, USA) using the diffuse reflectance interface. The sample holder had a diameter of 2 cm and contained ~2 g of soil material, which was gently levelled with a pestle before taking the handheld measurements. The Agilent 4000-series portable MIR instruments have recently been shown to deliver comparable calibration accuracies to reference laboratory benchtop spectrometers on pre-treated samples (Soriano-Disla et al., 2017; Hutengs et al., 2018). Measurements on dried and ground soil material were therefore carried out with the same instrument as on the field-moist soils. The handheld instrument measured diffuse reflectance in the 4000–650 $cm^{-1}$ wavenumber range (~2500–15,000 nm) with a spectral resolution of 4 $cm^{-1}$ (~2.5 nm and ~100 nm at the respective endpoints of the spectral range), sampled at ~2 $cm^{-1}$ increments; its spot diameter is <2 mm, corresponding to a measured sample area <0.03 $cm^2$. On the finely ground soil material, two replicates with 64 co-added scans were measured and combined into a single MIR spectrum. On the field-moist samples, which were not homogenized through grinding, we collected four replicate measurements with 32 co-added scans, each on distinct subsamples. The MIR spectrometer was calibrated with a manufacturer-provided gold-plated reference cap every ~10 min. For laboratory analysis, more elaborate setups for the handheld MIR instrument, with potential gains in spectral accuracy, would be possible (Soriano-Disla et al., 2017); we opted for the manual operation of the instrument because on-site analysis is among the greatest potential advantages of these instruments and our approach readily facilitates field application.

While the VNIR data were collected on different instruments for field-moist and pre-treated soils, in contrast to the MIR data, previous studies showed that the effect of instrument-type on spectroscopic

calibrations (Knadel et al., 2013; Gholizadeh et al., 2021; Hutengs et al., 2018; Soriano-Disla et al., 2017) is minor compared to the effects of soil condition (field-moist vs. pre-treated) and spectral range (VNIR vs. MIR) (Hutengs et al., 2019). In the following, we will therefore treat the Agilent 4300, ASD FieldSpec 4 and FOSS XDS measurements as representative of their respective spectral range for a given soil condition.

## 2.4 Multivariate calibration and statistical analysis

### *2.4.1 PLSR calibrations of VNIR and MIR spectral data*

We used partial least squares regression (PLSR; Wold et al., 2001; Wehrens, 2011) to calibrate predictive models for soil physicochemical and microbial properties. Prior to PLSR calibration, VNIR and MIR spectra were pre-processed with multiplicative scatter correction (MSC), standard normal variate transformation (SNV) and L1-norm vector normalization, each applied to reflectance spectra (R) and spectra converted to apparent absorbance units with $A = \log_{10}(1/R)$, respectively. This resulted in a total of eight spectral datasets for each spectral range, including the original reflectance and absorbance data. We applied these standard spectral pre-processing techniques to remove undesired systematic variations such as baseline shifts and drift from the spectra, which affect the predictive accuracy of PLSR models ( Rinnan et al., 2009). As overall cross-validated predictive accuracies were very similar for each pre-processing technique but depicted different random error patterns, we combined the output of the individual eight PLSR calibrations into a single ensemble estimate for each soil property and spectral range:

$$\hat{y}_{i,SPEC} = \frac{\sum_{k=1}^{m} \hat{y}_{i,k}}{m},$$

where *SPEC* is the spectral range (VNIR or MIR), $\hat{y}_{i,k}$ is the PLSR prediction for sample *i* with spectral pretreatment *k*, and *m* is the number of spectral pretreatments.

We further combined VNIR and MIR estimates through a precision-weighted average to generate combined VNIR/MIR estimates that incorporate the spectral information acquired by each instrument and take the accuracy of individual sensor models into account:

$$\hat{y}_{i,VNIR/MIR} = \frac{w_{VNIR} \cdot \hat{y}_{i,VNIR} + w_{MIR} \cdot \hat{y}_{i,MIR}}{w_{VNIR} + w_{MIR}},$$

where $w = (RMSE_{cal})^{-1}$, i.e., the reciprocal of the root mean square error for a given soil property in 10-fold cross-validation, is the overall precision of the VNIR and MIR model, respectively.

We averaged the individual estimates of VNIR and MIR models as this approach has recently been shown to be superior to the merging of VNIR and MIR data into a single spectrum prior to calibration (Xu et al., 2019). High-level data fusion approaches also generalize well to multi-sensor applications that could combine VNIR and MIR spectra with, for example, data from XRF (X-ray fluorescence; O'Rourke et al., 2016) and LIBS (laser-induced breakdown spectroscopy; Xu et al., 2019) sensors.

For model calibration and validation, we randomly divided the dataset of n = 80 soils into a training and a test set. PLSR models were calibrated on the training set with $n_{train}$ = 40 soil samples. The number of latent variables to retain was determined by 10-fold cross-validation on the training samples. Predictions from the PLSR models were then evaluated on an independent test set which comprised the remaining $n_{test}$ = 40 samples.

As the randomized splitting into calibration and test set may favour either the VNIR or MIR spectral range or lead to better calibrations for some soil properties simply by chance, we repeated this procedure over 100 runs with different randomized train/test splits and report averages from the resulting distributions of various accuracy statistics.

VNIR and MIR models were calibrated for OC, N, IC, sand and clay content, as well as the microbial biomasses derived from the PLFA biomarkers. Soil pH and moisture content were excluded as their lab-analytical determination is comparatively quick and inexpensive; in addition, specialized compact proximal sensors to measure these properties in the field are readily available (Adamchuk et al., 2018).

We evaluated PLSR model performance for each soil property on the independent test sets with the standard error statistics reported in soil spectroscopy studies (e.g., Hutengs et al., 2019), including root mean square error (RMSE), the coefficient of determination ($R^2$), mean error or bias (ME), the ratio of performance to deviation (RPD) and the ratio of performance to interquartile distance (RPIQ).

RMSE differences for relevant combinations of spectral data (VNIR, MIR, VNIR/MIR) and soil pretreatment (field-moist, dried/ground) across all soil properties were tested for statistical significance using the Wilcoxon signed-rank test. This includes the three possible comparisons between spectral data models within each soil pretreatment and three further comparisons between dried/ground and field-moist models for VNIR, MIR and VNIR/MIR data, respectively. The results of the pairwise comparisons are provided as Supplementary Material (S1). For individual comparisons highlighted in the text, we used a Bonferroni-corrected significance threshold $\alpha^*$ for $m$ = 9 comparisons of interest across each soil property given by $\alpha^* = \alpha/m$; the adjusted traditional significance level $\alpha$ = 0.05 would thus correspond

to (rounded down) $\alpha^* = 0.005$; pairwise RMSE differences with $p < 0.005$ were thus considered statistically significant.

Multivariate PLSR calibrations, VNIR and MIR spectral data pre-processing and further computations were carried out in the R statistical computing software (R Core Team, 2020) using the "chemometrics" ( Filzmoser and Varmuza, 2017) and "prospectr" (Stevens and Ramirez-Lopez, 2020) packages.

### *2.4.2 Multiple linear regression and linear mixed effects models*

Multiple linear regression (MLR) models were used to estimate soil microbial properties derived from PLFA analysis with the available physicochemical soil data (OC, N, IC, sand, clay, pH, $H_2O$). The comparison between MLR estimation accuracies and the VNIR/MIR PLSR models (Section 3.3) allows drawing conclusions as to whether the soil reflectance data contain additional information regarding PLFA-derived microbial biomasses beyond correlations with physicochemical bulk soil properties (Ludwig et al., 2015).

Eigendecomposition and variance inflation factor (VIF) analysis of physicochemical soil data indicated high collinearity in the MLR design matrix, which can make the least squares estimates of the regression coefficients unstable (Faraway, 2014). MLR models were therefore fitted with ridge regression (Hoerl and Kennard, 1970; James et al., 2013). Ridge regression computations were carried out with the R package "glmnet" (Friedman et al., 2010). We evaluated MLR models in the same randomized calibration-validation procedure described above for the VNIR and MIR PLSR models.

We additionally fitted simple linear mixed effects (LME) models for OC, $PLFA_{BAC}$, $PLFA_{FUN}$ and F:B with the two main whole-plot treatments of the Jena Experiment as explanatory factors (number of sown plant species (SP) and number of plant functional groups (FG)) to investigate whether estimates from VNIR/MIR PLSR models provide comparable results to the laboratory analytical data when analyzing treatment effects (Ball et al., 2020). LME models were constructed with the "lme4" package in R (Bates et al., 2015). The general structure was: Response ~ SP + FG + SP × FG + (1|BLOCK), where BLOCK refers to the blocks in the Jena Experiment's layout, included as a random effect. The 60-species plots are not replicated within the experimental blocks (Fig. 1) and were excluded from the LME analysis. Fixed effect terms were added sequentially to the model as prescribed by the experimental design in the order SP, FG, SP × FG. Model selection was carried out by considering the Akaike Information Criterion (AIC) and the statistical significance of the added terms. Statistical significance of the added terms was

calculated based on the likelihood ratio statistic of the nested models in sequence using the parametric bootstrap method implemented in the "pbkrtest" R package (Halekoh and Højsgaard, 2014).

# 3 Results

## 3.1 Descriptive statistics of soil physicochemical and microbial properties

Soils from the Jena Experiment (Table 1) had moderate OC contents of ~20 g/kg on average, ranging from 12.9–32.4 g/kg with substantial variation (SD = 3.5 g/kg) due to the nature of the experimental site. IC content was substantial (mean = 16.6 g/kg) and variation in soil pH limited accordingly (7.0–7.8), with ~75% of the samples falling into the neutral pH range. Soil texture ranged from sandy loam to silt loam following a gradient perpendicular to the Saale river with sand contents of up to 48% on experimental plots near the river and only 3% on the plots farthest away. Microbial biomass varied between 6.7 and 17.0 µg/g; $PLFA_{MIC}$ made up about half of all extracted PLFAs. Soil microbial community composition was dominated by bacteria with F:B ratios between 0.13 and 0.31 across the site. G+ bacterial biomass was more abundant than G− bacterial biomass by a factor of ~6.5 on average.

**< insert Table 1 about here >**

Soil physicochemical and microbial properties were significantly intra- and inter-correlated across the site (Fig. 3, Supplementary Material S2). OC was strongly correlated with total N ($r$ = 0.86) and showed weak correlations with sand ($r$ = −0.25) and clay content ($r$ = 0.27). PLFA-derived microbial biomasses correlated well with OC ($r$ = 0.61–0.73), except for the more moderate correlation with $PLFA_{FUN}$ ($r$ = 0.47). PLFA quantities, with the exception of $PLFA_{FUN}$, were further strongly correlated among each other ($r$ = 0.91–0.99). Correlations between $PLFA_{FUN}$ and the other PLFA fractions were generally weaker ($r$ = 0.74–0.90). Both PLFA biomasses and OC correlated well with soil moisture content ($r$ = 0.57–0.68); correlations between soil pH and PLFA biomasses were generally weak ($r \leq 0.25$). F:B ratios across the site were negatively correlated with sand content ($r$ = −0.64) and positively with IC ($r$ = 0.68) and clay ($r$ = 0.46); correlations of F:B with soil texture and IC were larger than with pH ($r$ = 0.24), soil moisture ($r$ = 0.28) or C:N ratios ($r$ = −0.23). OC and F:B ratios were not significantly correlated.

**< insert Figure 3 about here >**

### 3.2 VNIR and MIR spectral measurements

Soil reflectance spectra collected on pre-treated sample material in the VNIR and MIR (Fig. 4a and b) depicted organic-affected but otherwise minimally altered (low Fe oxide absorption at ~650 and 900 nm) mineral soils. MIR spectra indicated intermediate clay contents (kaolinite and smectite clays, ~3695 $cm^{-1}$ and ~3620 $cm^{-1}$) and moderate organic matter content (aliphatic C–H stretch, 3000–2800 $cm^{-1}$). Substantial amounts of soil carbonate were evident from the spectra (broad absorption peak with a shoulder at ~2500 $cm^{-1}$); spectral variation from 2000 to 1790 $cm^{-1}$ indicated significant variability in silica (quartz/sand) content (Fig. 4b). The VNIR range exhibited smaller absorption features primarily due to carbonate overtones (~2350 nm), overtone and combination bands of water and hydroxyl (OH) in water-bearing minerals (~1400 nm, ~1900 nm) and combinations of metal-OH and OH vibrations in clay minerals (2200–2300 nm) (Fig. 4a).

**< insert Figure 4 about here >**

For field-moist soils, the measured VNIR and MIR reflectance curves changed substantially. Total reflectance was lowered by about 50% on average, and soil spectra in both regions were more variable ( Fig. 4c and d). In the VNIR, field-moist spectral data additionally depicted a flatter reflectance slope in the visible range (500–750 nm) and strong absorptions due to soil water at ~1400 nm and ~1900 nm ( Fig. 4c). In the MIR, the absorption features described for the pre-treated soils were still identifiable but significantly attenuated. The wide OH-band centred at ~3400 $cm^{-1}$ for dried soil broadened further, and spectral variation increased from 3000 $cm^{-1}$ to 1750 $cm^{-1}$ (Fig. 4d).

### 3.3 VNIR and MIR PLSR calibrations for soil physicochemical and microbial properties

#### *3.3.1* Soil physicochemical properties

Soil physicochemical properties could be estimated with high accuracy ($R2 \geq 0.82$) on pre-treated samples (Table 2), except for clay content ($R^2 = 0.67–0.72$) and total N in the VNIR range ($R^2 = 0.73$). MIR estimates were more accurate than VNIR estimates, especially for OC ($\Delta$RMSE = 23%, $p < 0.001$), IC ($\Delta$RMSE = 46%, $p < 0.001$) and N ($\Delta$RMSE = 22%, $p < 0.001$). Differences between VNIR and MIR for sand and clay content were marginal and not statistically significant ($\Delta$RMSE ~2%; $p_{Sand} = 0.033$, $p_{Clay} = 0.211$). Combined VNIR/MIR estimates achieved the best estimation results overall. Improvements were small ($\Delta$RMSE = 4–11%, $p < 0.001$) but consistent across all estimated soil properties except for N ($\Delta$RMSE ~0%, $p = 0.129$).

**< insert Table 2 about here >**

PLSR calibrations on field-moist soils were overall less accurate but not for all soil properties. Estimation accuracy for both VNIR and MIR data decreased notably for OC and IC (ΔRMSE = 51–61% and 20–48%, $p < 0.001$). For N, MIR accuracy decreased by ~11% ($p < 0.001$), while VNIR accuracy improved slightly (ΔRMSE = 4%, $p = 0.004$). Estimates of sand and clay content from field-moist soils were not significantly different from pre-treated samples (ΔRMSE = 2–4%, $p = 0.050$–$0.574$). Similar to the different performances on pre-treated samples, MIR spectra gave more accurate estimates than VNIR data for all considered soil properties (ΔRMSE = 3–34%); for clay content, however, the RMSE difference was not statistically significant ($p = 0.011$). Combined VNIR/MIR estimates were also consistently more accurate than models for each individual spectral region showing further improvements (ΔRMSE = 4–15%, $p < 0.001$) comparable in magnitude to the models for pre-treated soils.

Direct comparison of VNIR/MIR estimates and laboratory reference values showed that estimation errors were generally consistent and unbiased over the calibrated range for all soil physicochemical properties except clay content (Supplementary Material S3). The comparatively inaccurate estimations for clay content resulted from a systematic underestimation of higher values. For clay contents >23%, the VNIR/MIR estimates had little predictive value. PLSR calibrations on field-moist soils also appeared to underestimate the highest OC values systematically.

### *3.3.2 PLFA-derived soil microbial properties*

Estimation accuracies of soil microbial properties (Table 3) were less accurate ($R^2 = 0.47$–$0.72$) compared to soil physicochemical properties (Section 3.3.1). On dried sample material, MIR calibrations for all PLFA quantities were more accurate than VNIR models (ΔRMSE = 4–10%, $p \leq 0.002$), and combined VNIR/MIR estimates further improved accuracy slightly (ΔRMSE = 3–7%, $p < 0.001$). On field-moist soils, however, VNIR estimates were more accurate than MIR estimates for all PLFA quantities (ΔRMSE = 5–19%, $p < 0.001$), except for $PLFA_{G+}$ (ΔRMSE ~0%, $p = 0.513$). In the MIR, estimation accuracy decreased substantially compared to the pre-treated sample material (ΔRMSE = 12–28%, $p < 0.001$). In contrast, differences between VNIR estimates on field-moist and pre-treated soils were not consistent (ΔRMSE = −7 to +8%). For $PLFA_{TOT}$, $PLFA_{MIC}$ and $PLFA_{BAC}$, the accuracy differences were not statistically significant (ΔRMSE = −1 to +3%, $p = 0.213$, 0.547 and 0.008, respectively). Combined VNIR/MIR estimates still yielded the best results with moderate but consistent improvements in estimation accuracy for all PLFA quantities (ΔRMSE = 2–10%, $p < 0.001$). Compared to combined VNIR/MIR estimates on pre-treated sample material, estimates of PLFA quantities on field-moist soil were only slightly less accurate (ΔRMSE = 4–9%, $p < 0.001$).

**< insert Table 3 about here >**

The comparison of VNIR/MIR estimates and laboratory reference values across all validation samples (Fig. 5) showed that estimation errors for soil microbial properties were consistent and mostly unbiased across the calibrated range. Some bias for estimates in the tails of the soil property distributions was apparent, i.e., under- and overestimation of high and low values, respectively, and slightly more pronounced for calibrations on field-moist soils. Apart from that, differences in estimation error distributions between pre-treated and field-moist PLSR calibrations appeared negligible.

**< insert Figure 5 about here >**

Despite relatively moderate estimation accuracies, VNIR/MIR estimates could mostly reproduce the conditional distributions of soil microbial properties for the main treatments of the Jena Experiment (Fig. 6). The distributions of selected soil properties (OC, $PLFA_{BAC}$, $PLFA_{FUN}$, F:B) by plant species richness and functional group richness for lab-analytical data showed that OC, $PLFA_{BAC}$, $PLFA_{FUN}$ increased with SP (Fig. 6a), and to a lesser degree FG (Fig. 6b), whereas the F:B ratio remained relatively constant. The VNIR/MIR estimates reproduced these trends well overall, but the differences between the most extensive treatment contrasts (e.g. monocultures vs. 16-species plots) were smaller in the spectral data.

**< insert Figure 6 about here >**

Additionally, we analyzed whether VNIR/MIR estimates could be used to detect plant treatment effects on OC, $PLFA_{BAC}$, $PLFA_{FUN}$ and F:B by comparing LMEs that used the laboratory-analytical data as input (Table 4a) with models fitted with the spectroscopic estimates (Table 4b). For OC, $PLFA_{BAC}$ and $PLFA_{FUN}$, the VNIR/MIR estimates yielded the same model structure and similar effect sizes as the lab-analytical data.

**< insert Table 4a about here >**

**< insert Table 4b about here >**

For lab-analytical data, SP explained a statistically significant amount of variation, after accounting for the experiment's block layout, for OC ($\Delta AIC = -18.2$, $p < 0.001$), $PLFA_{BAC}$ ($\Delta AIC = -41.1$, $p < 0.001$), $PLFA_{FUN}$ ($\Delta AIC = -41.8$, $p < 0.001$). In contrast, including FG did not improve model fit significantly for either OC ($\Delta AIC = 3.1$, $p = 0.394$), $PLFA_{BAC}$ ($\Delta AIC = 0.3$, $p = 0.126$) or $PLFA_{FUN}$ ($\Delta AIC = 5.0$, $p = 0.793$). Fitting the LMEs with VNIR/MIR estimates instead also indicated statistically significant contributions of SP for OC ($\Delta AIC = -21.2$, $p < 0.001$), $PLFA_{BAC}$ ($\Delta AIC = -36.8$, $p < 0.001$), $PLFA_{FUN}$ ($\Delta AIC = -36.9$, $p < 0.001$) and no statistically significant overall contribution of FG (OC: $\Delta AIC = 3.0$, $p = 0.394$; $PLFA_{BAC}$: $\Delta AIC = 5.0$, $p = 0.801$;

$PLFA_{FUN}$: ΔAIC = 4.1, $p$ = 0.584). Effect sizes were similar in direction and magnitude but overall smaller when the VNIR/MIR data was used in the analysis.

For analysis of the F:B ratio, however, VNIR/MIR estimates were not accurate enough. Lab-analytical data indicated statistically significant contributions of both SP (ΔAIC = −5.6, $p$ = 0.009) and FG (ΔAIC = −2.9, $p$ = 0.030), but not their interaction (ΔAIC = 6.2, $p$ = 0.313). F:B increased with SP and decreased with FG. VNIR/MIR estimates of the F:B ratio led to the same model structure (SP: ΔAIC = −8.9, $p$ = 0.002; FG: ΔAIC = −3.7, $p$ = 0.021; SP × FG: ΔAIC = 4.2, $p$ = 0.199). However, the model coefficients diverged in size and direction, leading to different conclusions about the impact of FG on the F:B ratio. If the VNIR/MIR estimates were used instead, contributions of both above-ground treatment factors were positive and close to zero.

### 3.4 Predictive mechanisms for PLSR calibrations of soil microbial properties

The evaluation of correlation profiles for VNIR and MIR spectra (Fig. 7) showed that soil physicochemical and microbial properties in both spectral ranges had high correlations over a wide range of reflectance bands. Correlation profiles for soil microbial properties were overall very similar. Only $PLFA_{FUN}$, which had a lower correlation with the other PLFA quantities (Section 3.1), depicted a slightly deviating correlation pattern. The observed correlation patterns for soil microbial properties mostly matched those of soil physicochemical properties. High correlations between PLFA quantities and OC and N, for example, were mirrored in similar spectral correlation profiles, as was the stronger association between $PLFA_{FUN}$ and IC and sand content. The observed correlation patterns differed substantially between spectral measurements on pre-treated and field-moist sample material. Correlations over individual spectral ranges were reversed in some cases (e.g., over the main OH band ~3400 $cm^{-1}$ in the MIR or the metal-OH absorption range 2200–2300 nm in the VNIR). However, the high overall similarity among correlation patterns was also evident for the field-moist samples, except for sand and clay, which diverged substantially compared to the pre-treated soils.

**< insert Figure 7 about here >**

Due to the high agreement of spectral correlation patterns between soil physicochemical and microbial properties, we investigated if MLRs with OC, N, IC, pH, soil moisture, sand and clay content could estimate PLFA quantities accurately (Table 5). MLR models accounted for ~50% of the variation in the soil microbial properties with estimation accuracies between $R^2$ = 0.49 and 0.55. In comparison, VNIR/MIR calibrations on field-moist samples explained ~13% more variance ($R^2$ = 0.61–0.68), on pre-

treated samples ~17% ($R^2$ = 0.66–0.72). MLR estimates were also less accurate than PLSR calibrations for individual spectral ranges and sample pretreatments, except for MIR data collected on field-moist samples, which gave comparable results ($R^2$ = 0.47–0.59).

**< insert Table 5 about here >**

Apart from the correspondence between correlation patterns of soil microbial and physicochemical properties, spectral correlation profiles also depicted strong similarities among the PLFA quantities. Analysis of ratio indices, which tend to remove mutually shared underlying correlations, calculated from the VNIR/MIR estimates (Table 6) showed that these were substantially less accurate than estimates for the corresponding input soil properties. $R^2$ values for MIC:OC, F:B and G+:G− were 0.43, 0.52 and 0.33, respectively, for calibrations on pre-treated samples. Accuracy for the ratios was lower for field-moist sample material ($R^2$ = 0.21–0.43). VNIR/MIR calibrations on pre-treated samples still accounted for considerably more variance in the ratio indices than MLRs. However, MLRs provided comparable results ($R^2$ = 0.16–0.42) to VNIR/MIR PLSR calibrations on the field-moist sample material.

**< insert Table 6 about here >**

# 4 Discussion

## 4.1 Associations of soil physicochemical and microbial properties at the Jena Experiment site

The soil microbial community at the Jena Experiment site was significantly associated with the physicochemical soil environment. Soil pH, the quantity and quality of organic matter (e.g., OC, N), soil moisture and soil texture (e.g., sand and clay content) are generally among the main factors influencing soil microbial communities (Fierer, 2017). Previous studies at the Jena Experiment have shown that changes in soil microbial community structure (e.g., $PLFA_{BAC}$, $PLFA_{FUN}$, F:B) have likely been driven by the quality and quantity of organic resources varying with plant diversity (Lange et al., 2015; Mellado-Vázquez et al., 2016) causing a significant plant diversity effect on soil microbial properties and communities (Eisenhauer et al., 2010, 2017). The positive relationships we found between soil microbial biomass and soil moisture and clay content are also in line with previous findings at the Jena Experiment site (Eisenhauer et al., 2010; Lange et al., 2014).

Strong associations between soil physicochemical characteristics (OC, N and moisture) and PLFA-derived soil microbial properties across multiple land-use types have also recently been reported by Zhang et al. (2016). Contrary to other studies (Zhang et al., 2016; Xia et al., 2020), the influence of soil

pH on microbial properties was relatively limited at the Jena Experiment site, possibly due to the narrow pH range buffered above the neutral point through the presence of significant amounts of $CaCO_3$ in the site's soils.

### 4.2 VNIR and MIR spectral measurements with portable instruments

The collected VNIR and MIR spectra captured the major compositional features of the Jena Experiment site's soils, i.e., moderate OC contents, substantial amounts of IC in the soils and predominantly loamy soil texture. For pre-treated samples, VNIR and MIR diffuse reflectance spectra have been described in detail elsewhere, including key absorption features of organics and minerals and possible band assignments (Stenberg et al., 2010; Parikh et al., 2014).

Importantly, the spectral data we collected on soils in field condition (variable particle size and soil moisture) appeared to retain much of the relevant soil information in the form of significant absorption features. It is well known that variable water content impacts diffuse reflectance spectra significantly, especially in the MIR (Reeves, 2010; Stenberg, 2010; Nocita et al., 2013; Janik et al., 2016), where water absorbance is much stronger than in the VNIR, highly non-linear and can lead to severe spectral distortions (Janik et al., 2016). The MIR data we collected with the handheld instrument on field-moist soils, however, depicted higher reflectance values at ~4000 $cm^{-1}$, where the spectral ranges from both instruments connect, likely due to differences in instrument technology and sampling setup.

For the VNIR instrument, the contact probe attachment provides a standardized measurement method to collect data on loose soil samples. The MIR instrument, on the other hand, was not explicitly designed for soil analysis and required more care during data collection, especially on soils in field condition. For field-moist soils, compacting the samples in a small sample holder to minimize pore space and increase signal strength was necessary, for example, to obtain high-quality spectra with relatively little noise. This may have also inadvertently benefitted MIR measurements by breaking up soil aggregates to make them accessible to the IR beam (Forrester et al., 2015).

It is important to note that the impact of soil moisture on MIR spectra depends on both the amount of soil water present and its interaction with the soil matrix (Janik et al., 2016; Silvero et al., 2020). Clay-rich soils, for example, tend to cause minimal distortion at moisture contents typical of field conditions compared to high sand soils (Janik et al., 2016). While we did not observe any severe distortions in our MIR spectra, field analysis of MIR data should thus preferably be carried out at lower soil moisture levels. If permissible, air/sun-drying the sample material has been shown to work well and might be an

option to limit the confounding effects of soil moisture on spectra collected in the field (Reeves et al., 2010; Izaurralde et al., 2013).

## 4.3 Estimation accuracies of VNIR and MIR PLSR calibrations on pre-treated and field-moist soils

### *4.3.1 Soil physicochemical properties*

VNIR and MIR PLSR models gave accurate estimates of soil physicochemical properties on pre-treated sample material with better calibrations in the MIR, as expected, based on the vast body of VNIR and MIR soil spectroscopy literature (Stenberg et al., 2010; Soriano-Disla et al., 2014). More specifically, our results corroborate more recent findings on the performance of handheld MIR instruments, which have been shown to achieve quantitative calibrations of soil physicochemical properties comparable to established benchtop laboratory spectrometers (Soriano-Disla et al., 2017; Hutengs et al., 2018; Martínez-España et al., 2019; Janik et al., 2020).

The relatively moderate estimation accuracies for soil clay content compared to other studies (e.g., Ng et al., 2019) were somewhat unexpected, however, given the established spectral response of clay minerals in the VNIR and MIR (Nguyen et al., 1991; Parikh et al., 2014). Deviations between estimated and reference soil clay content possibly resulted from a mismatch between soil clay mineral content and the clay particle size fraction due to the presence of significant contributions of fine-grained calcite crystals (Kerry et al., 2009).

Combining VNIR and MIR PLSR estimates yielded small but consistent improvements in estimation accuracy for our data, in line with previous studies that combined spectral information from each range through various methods. This includes concatenating VNIR and MIR data into a single spectrum prior to modelling (Knox et al., 2015), merging VNIR and MIR data through the outer product of the spectral data matrices (Terra et al., 2019) and Bayesian model averaging of VNIR and MIR estimates (Xu et al., 2019).

PLSR calibrations on soils in field condition gave satisfactory results overall, although estimates for OC and IC were substantially less accurate than on pre-treated soils. Based on previous studies with VNIR instruments, decreased calibration accuracy on field-moist soils was expected (e.g., Stevens et al., 2006; Terhoeven-Urselmans et al., 2008; Kuang and Mouazen, 2011; Hong et al., 2018; Hutengs et al., 2018) as sample-wise variation in moisture tends to confound the relationships between the measured reflectance signal and the soil constituents of interest (Nocita et al., 2015). However, this effect is not

necessarily universal for all soil moisture levels, soil types and soil properties, as rewetting experiments have shown (Stenberg, 2010; Nocita et al., 2013). Similar to our findings, Marakkala Manage et al. (2018) recently demonstrated that soil moisture decreases VNIR calibrations of OC rather severely but had comparably little influence on estimates of sand and clay content.

MIR data has generally been expected to perform worse for the analysis of field-moist soils than the VNIR due to the more severe impact of soil water on the reflectance signal in the MIR (Reeves, 2010; Kuang et al., 2012). Interestingly, we found that the MIR instrument allowed more accurate PLSR estimates across all soil physicochemical properties for field-moist soils. For OC, this was in line with results we recently reported for in situ VNIR and MIR measurements on a set of finely-textured Chernozem soils (Hutengs et al., 2019). In contrast, Reeves et al. (2010) reported substantially less accurate estimates for OC and N when comparing VNIR and MIR calibrations on soils in field condition. For soil texture, Janik et al. (2020) recently showed that estimates of sand and clay content were significantly better on pre-treated than in-situ soils, unlike what we found here for the Jena Experiment site.

Given the complex interactions between soil texture and moisture content in the MIR (Janik et al., 2016), further case studies will be necessary to determine if MIR instruments generally allow improved estimates of soil physicochemical properties on field-moist soils and under which boundary conditions (e.g., soil types, moisture levels, particle size distribution). In this context, the fact that combined VNIR and MIR estimates also achieved the most accurate results on field-moist soils was promising, as it indicates that the synergistic use of VNIR and MIR instruments has the potential to significantly advance on-site soil spectroscopy.

#### *4.3.2 PLFA-derived soil microbial properties*

For PLFA-derived soil microbial properties, we found generally less accurate estimation accuracies for VNIR and MIR PLSR models than for soil physicochemical properties, which is in line with the available literature summarized by Soriano-Disla et al. (2014). In the VNIR, for example, previous studies reported calibration accuracies of $R^2$ ~0.62 to ~0.90 and $R^2$ ~0.58 to ~0.85 for microbial biomass C and ergosterol fungal biomarkers, respectively (Rinnan and Rinnan, 2007; Terhoeven-Urselmans et al., 2008; Heinze et al., 2013). Comparable results were reported for the MIR spectral region (Ludwig et al., 2008, 2015, 2016; Rasche et al., 2013). For PLFAs in particular, Rinnan and Rinnan (2007) reported $R^2$ values of 0.61 for $PLFA_{TOT}$ and $PLFA_{FUN}$ for VNIR calibrations of highly organic soils in a long-term climate

manipulation experiment. A more extensive set of PLSR calibrations for PLFAs in the NIR, comparable to our study, was reported by Zornoza et al. (2008) for arable and forest soils. They found cross-validated $R^2$ values of 0.91 for $PLFA_{TOT}$, 0.93 for $PLFA_{BAC}$, 0.77 for $PLFA_{FUN}$, and 0.60 and 0.91 for $PLFA_{G-}$ and $PLFA_{G+}$, respectively. In this context, it should be noted that $R^2$ scores for spectroscopic calibrations can strongly depend on the variation in the data. For a given soil property, $R^2$, i.e., the explained variation of the model estimates, increases with the standard deviation of the data given the same RMSE. While RMSEs also tend to increase when the calibrated soil property is more variable, datasets with greater variation have been shown to lead to generally higher $R^2$ scores (Stenberg et al., 2010). In Zornoza et al. (2008), coefficients of variation for PLFAs were between 0.63 and 0.85, considerably larger than for our dataset (0.19–0.28). The PLSR calibration results in our study were thus broadly in line with previously published reports.

VNIR and MIR models also performed better on pre-treated than on field-moist soils, which was not necessarily expected, given the clear relevance of soil state on the size, composition and activity of soil microbial communities (Soriano-Disla et al., 2014). Field-moist soils might thus have reasonably been expected to allow better calibrations for soil microbial properties than the heavily altered, dried and mechanically ground powder samples. A potentially more representative signal for soil microbial biomass in field-moist soils, however, might have been offset by variable water contents and particle size distributions contributing confounding spectral variation to the recorded reflectance data.

Notably, declines in PLSR calibration accuracy for soil microbial properties on field-moist soils were only moderate for VNIR and combined VNIR/MIR estimates compared to the pre-treated samples, unlike for OC. For the MIR instrument by itself, however, calibrations were substantially worse and less accurate than in the VNIR, in contrast to the results for all considered soil physicochemical properties. The origin of this discrepancy is unclear, as the MIR region generally contains more relevant spectral information related to soil mineralogical structure and organic matter quality (Stenberg et al., 2010; Parikh et al., 2014). More robust measurements with the VNIR instrument on field-moist soils would be a plausible explanation, although the soil water contents present in the dataset did not degrade MIR performance for the other soil properties. For soil microbial properties, however, the differences between the correlation patterns of field-moist and pre-treated soils were markedly less substantial in the VNIR than in the MIR. Accordingly, the relationship between the spectral signal and the soils' microbial properties may have been masked more strongly in the MIR as soil microbial properties are more dynamic in response to soil conditions, in particular soil moisture, which affects the MIR signal in a more complex manner. In this context, it is encouraging that the combined VNIR/MIR estimates yielded the

most accurate estimates again, despite the diverging results, highlighting the possible advantages of employing both VNIR and MIR instruments for field analyses.

The usefulness of VNIR/MIR estimates with a given accuracy is relatively challenging to assess for microbial quantities, in contrast to soil physicochemical properties. For OC, IC and soil texture, for example, absolute RMSE values on the order of ~1–2 g/kg and a few percentage points, respectively, can be considered accurate enough to act as a substitute for routine laboratory analyses in soil surveying (Seybold et al., 2019).

For $PLFA_{BAC}$, $PLFA_{FUN}$ and F:B, we therefore exemplarily tested if and how replacing routine laboratory-analytical data with VNIR/MIR estimates would change the conclusions drawn from statistical LME analyses for the Jena Experiment's plant treatments. Interestingly, we found that even moderately accurate VNIR/MIR estimates ($R^2$ ~0.6–0.7) could be sufficient to detect local treatment-level differences, as was the case for the effects of plant species richness and functional diversity on $PLFA_{BAC}$, $PLFA_{FUN}$ and OC. A similar finding was recently reported by Ball et al. (2020) for the effects of cover crop treatments on OC and N in particle size fractions. Accordingly, even PLSR models that would typically be considered inaccurate by soil spectroscopy standards may be sufficient to detect the impact of above-ground plant communities on soil microbial communities. At lower accuracies, detecting such effects is unlikely, however, as our LME analysis for the F:B ratio showed ($R^2$ = 0.43). For the F:B ratio, VNIR/MIR estimates yielded the same model structure, but model coefficients were incomparable with the LME results for the PLFA-derived F:B ratios.

### 4.4 Predictive mechanisms of soil microbial properties and their implications for VNIR and MIR analysis

The scope of predictive models in soil spectroscopy strongly depends on the mechanisms underlying the PLSR calibrations. For the Jena Experiment site, we found spectral correlation patterns between PLFA-derived quantities and physicochemical soil data (OC, N, IC, clay and sand contents) that matched the correlation structure between soil physicochemical and microbial properties, indicating that spectrally active soil constituents mediated successful VNIR/MIR estimations of soil microbial properties. This was further corroborated through the estimation of PLFA quantities with MLRs using physicochemical covariates, which achieved similar predictive accuracy to the VNIR/MIR models. These findings further underpin prevailing theories on successful VNIR/MIR calibrations of soil biological and

microbial properties (Cohen et al., 2005; Chodak et al., 2007; Rinnan and Rinnan, 2007; Zornoza et al., 2008; Rasche et al., 2013; Ludwig et al., 2015).

Earlier studies hypothesized that spectroscopic calibrations of soil biological and microbial properties are mediated by the capacity of VNIR and MIR spectroscopy to measure the quantity and quality of soil organic matter (Cohen et al., 2005; Chodak et al., 2007; Rinnan and Rinnan, 2007). Zornoza et al. (2008) , for example, reported that NIR calibrations of PLFA-based biomasses were only moderately more accurate than simple linear regressions with OC over a broad range of soil types in the Mediterranean. More recently, Ludwig et al. (2015, 2016) showed that linear regressions with spectrally active soil physicochemical properties were as predictive of microbial biomass C, N and the fungal biomarker ergosterol as MIR spectral data.

In contrast, we found that VNIR/MIR models consistently accounted for more variation in all PLFA-derived soil microbial properties, indicating that VNIR/MIR spectral data allow a more detailed characterization of the physicochemical soil environment relevant to soil microbial community composition than standard bulk soil properties. It was not clear, however, if VNIR/MIR models were more accurate due to their capability to assess substrate quality, i.e., distinguish labile and stabilized organic matter (Knox et al., 2015; Jaconi et al., 2019; Ricketts et al., 2020), or because the spectra merely contained more detailed information about the abiotic factors shaping the soil habitat, e.g. iron oxides, silicates, clay minerals (Stenberg et al., 2010; Parikh et al., 2014).

While individual PLFA quantities could be estimated fairly well, estimation accuracies for ratio parameters that capture the general composition of soil microbial communities (F:B, G+:G−) were markedly less accurate for both VNIR/MIR and MLR models; likely in part due to VNIR/MIR models relying on mutually shared correlations for estimations of individual PLFA quantities, as shown by the strong similarities in correlation profiles. The calculation of ratios removes these common associations, e.g., the scaling of all biomasses with OC. At the same time, F:B and G+:G- also depicted considerably less variation than the individual PLFA quantities, as the F:B ratio was dominated by bacterial biomass, which, in turn, was mostly made up of G+ bacteria. Accordingly, the capacity of VNIR/MIR data to capture variation in soil microbial communities may improve over larger environmental gradients, where strong links of soil biota to the prevailing abiotic soil environment exist. Yang et al. (2019), for example, recently found that VNIR data could contribute substantially to the mapping of regional-scale bacterial abundance and diversity across Australia.

VNIR/MIR models primarily leveraging associations between soil microbial properties and spectrally active physicochemical soil constituents is of crucial importance, in particular for the potential on-site analysis of soils in field condition. In this regard, our findings suggest that soil spectroscopy can provide an efficient tool to fill in-sample data gaps or improve the spatial mapping of microbial communities ( Rasche et al., 2013) when robust correlations between soil microbial properties and physicochemical soil data are present.

Out-of-sample predictions (calibration transfer), on the other hand, e.g., for different soil samples or time periods, cannot be expected to be accurate without further re-calibration as the underlying correlation structure between highly dynamic soil microbial communities and the relatively static physicochemical soil environment could easily change and render VNIR/MIR estimates unreliable. The issue of calibration transfer is further exacerbated on field-moist soils due to the moisture-dependent shifts in correlation patterns we have shown here, and which have also recently been demonstrated in rewetting experiments (Silvero et al., 2020). Application of VNIR/MIR models on soils in field condition would thus be further restricted to data collected under the same environmental conditions to ensure that the calibration adequately covers all relevant combinations of soil properties and moisture levels.

More extensive re-calibration data requirements for VNIR/MIR models arguably diminish the capacity of soil spectroscopy to acquire quantitative soil data efficiently. For pre-treated samples and physicochemical standard soil parameters, VNIR and MIR soil spectroscopy have increasingly focused on the integration of existing soil spectral libraries into local calibrations to keep additional calibration data requirements to a minimum (e.g., Wetterlind and Stenberg, 2010; Nocita et al., 2014; Terra et al., 2015; Seidel et al., 2019; Seybold et al., 2019). The development or expansion of soil spectral libraries with soil microbial properties and VNIR and MIR measurements at representative moisture levels could thus represent a significant step in the operational use of VNIR and MIR analyses on soils in field condition.

## 5 Conclusion

Here we presented the first comprehensive analysis of soil physicochemical and microbial properties with portable VNIR and MIR instruments in the framework of a long-term grassland biodiversity experiment. Our findings highlight the capabilities of soil spectroscopy to analyze physicochemical soil composition and associated soil microbial properties, including potential for on-site applications under field conditions and emphasize the synergistic use of current portable VNIR and MIR spectrometers. We

suggest that soil ecological studies could successfully integrate VNIR and MIR analysis to fill data gaps in the spatial analysis of soil microbial communities or by characterizing the underlying soil habitat in its physicochemical composition, which would also be possible without explicit calibrations to analytical reference data.

Several critical issues regarding the field application of soil spectroscopic analysis remain to be addressed by future studies. While we could detect some effects of plant community diversity and composition on soil microbial biomasses with VNIR/MIR analysis, the detection of treatment effects is complicated by the additional uncertainty in the VNIR/MIR estimates, which increases the detection threshold for treatment differences and thus makes detecting treatment effects that are small relative to the achievable calibration accuracy more difficult. The dynamic nature of soil microbial communities, e.g., short-term responses to variations in temperature or moisture, would also restrict the application of calibrated VNIR/MIR models that depend on sample-specific correlations with soil physicochemical properties. Establishing soil spectral libraries with field data and spectra collected at representative moisture levels will probably be necessary to keep requirements for new reference data to a minimum and facilitate operational use of VNIR and MIR spectroscopy in the field.

## Declaration of competing interest

The authors declare that they have no known competing financial interests or personal relationships that could have appeared to influence the work reported in this paper.

## Acknowledgements

We gratefully acknowledge the support of the German Centre for Integrative Biodiversity Research (iDiv) Halle-Jena-Leipzig, funded by the German Research Foundation (DFG – FZT 118, 202548816). This project has been conducted in the framework of the iDiv Flexpool – an internal funding mechanism of iDiv. We like to thank the technical staff of the Jena Experiment for their work in maintaining the experimental field site and also the many student helpers for the weeding of the experimental plots and support during the soil sampling. The Jena Experiment is funded by the German Research Foundation (DFG; FOR 456, FOR 1451, FOR 5000).

## Appendix A Supplementary data

Supplementary data to this article can be found online at https://doi.org/10.1016/j.soilbio.2021.108319.

## References


Adamchuk, V., Ji, W., Viscarra Rossel, R.A., Gebbers, R., Tremblay, N., 2018. Proximal soil and plant sensing. In: Shannon, D.K., Clay, D.E., Kitchen, N.R. (Eds.), Precision Agriculture Basics. American Society of Agronomy, Madison, pp. 119–140.

Ball, K.R., Baldock, J.A., Penfold, C., Power, S.A., Woodin, S.J., Smith, P., Pendall, E., 2020. Soil organic carbon and nitrogen pools are increased by mixed grass and legume cover crops in vineyard agroecosystems: detecting short-term management effects using infrared spectroscopy. Geoderma 379, 114619. doi:10.1016/j.geoderma.2020.114619.

Bardgett, R.D., van der Putten, W.H., 2014. Belowground biodiversity and ecosystem functioning. Nature 515 (7528), 505–511. doi:10.1038/nature13855.

Bates, D., Mächler, M., Bolker, B., Walker, S., 2015. Fitting linear mixed-effects models using lme4. Journal of Statistical Software 67 (1), 1–48. doi:10.18637/jss.v067.i01.

Chaparro, J.M., Sheflin, A.M., Manter, D.K., Vivanco, J.M., 2012. Manipulating the soil microbiome to increase soil health and plant fertility. Biology and Fertility of Soils 48 (5), 489–499. doi:10.1007/s00374-012-0691-4.

Chodak, M., Niklińska, M., Beese, F., 2007. Near-infrared spectroscopy for analysis of chemical and microbiological properties of forest soil organic horizons in a heavy-metal-polluted area. Biology and Fertility of Soils 44 (1), 171–180. doi:10.1007/s00374-007-0192-z.

Classen, A.T., Sundqvist, M.K., Henning, J.A., Newman, G.S., Moore, J.A.M., Cregger, M.A., Moorhead, L.C., Patterson, C.M., 2015. Direct and indirect effects of climate change on soil microbial and soil microbial-plant interactions: What lies ahead? Ecosphere 6 (8), 1–21. doi:10.1890/ES15-00217.1.

Cohen, M.J., Prenger, J.P., DeBusk, W.F., 2005. Visible-near infrared reflectance spectroscopy for rapid, nondestructive assessment of wetland soil quality. Journal of Environmental Quality 34 (4), 1422–1434. doi:10.2134/jeq2004.0353.

Dassen, S., Cortois, R., Martens, H., de Hollander, M., Kowalchuk, G.A., van der Putten, W.H., De Deyn, G.B., 2017. Differential responses of soil bacteria, fungi, archaea and protists to plant species richness and plant functional group identity. Molecular Ecology 26 (15), 4085–4098. doi:10.1111/mec.14175.

DIN ISO 10390, 2005. Bodenbeschaffenheit - Bestimmung des pH Wertes. Beuth Verlag, Berlin ISO 10390.

DIN ISO 10693, 2014. Bodenbeschaffenheit - Bestimmung des Carbonatgehaltes - Volumetrisches Verfahren. Beuth Verlag, Berlin ISO 10693.

Eilers, K.G., Debenport, S., Anderson, S., Fierer, N., 2012. Digging deeper to find unique microbial communities: the strong effect of depth on the structure of bacterial and archaeal communities in soil. Soil Biology and Biochemistry 50, 58–65. doi:10.1016/j.soilbio.2012.03.011.

Eisenhauer, N., Beßler, H., Engels, C., Gleixner, G., Habekost, M., Milcu, A., Partsch, S., Sabais, A.C.W., Scherber, C., Steinbeiss, S., Weigelt, A., Weisser, W.W., Scheu, S., 2010. Plant diversity effects on soil microorganisms support the singular hypothesis. Ecology 91 (2), 485–496. doi:10.1890/08-2338.1.

Eisenhauer, N., Lanoue, A., Strecker, T., Scheu, S., Steinauer, K., Thakur, M.P., Mommer, L., 2017. Root biomass and exudates link plant diversity with soil bacterial and fungal biomass. Scientific Reports 7 (1), 1–8. doi:10.1038/srep44641.

Ettema, C.H., Wardle, D.A., 2002. Spatial soil ecology. Trends in Ecology & Evolution 17 (4), 177–183. doi:10.1016/s0169-5347(02)02496-5.

Faraway, J.J., 2014. Linear Models with R. CRC Press, Boca Raton, FL.

Fierer, N., 2017. Embracing the unknown: disentangling the complexities of the soil microbiome. Nature Reviews Microbiology 15 (10), 579–590. doi:10.1038/nrmicro.2017.87.

P. Filzmoser, K. Varmuza. Chemometrics: Multivariate statistical analysis in chemometrics. R package version 1.4.2. https://CRAN.R-project.org/package= chemometrics, 2017.

Forrester, S.T., Janik, L.J., Soriano-Disla, J.M., Mason, S., Burkitt, L., Moody, P., Gourley, C.J.P., McLaughlin, M.J., 2015. Use of handheld mid-infrared spectroscopy and partial least-squares regression for the prediction of the phosphorus buffering index in Australian soils. Soil Research 53 (1), 67–80. doi:10.1071/sr14126.

Friedman, J., Hastie, T., Tibshirani, R., 2010. Regularization paths for generalized linear models via coordinate descent. Journal of Statistical Software 33 (1), 1. doi:10.18637/jss.v033.i01.

Frostegård, Å., Tunlid, A., Bååth, E., 1991. Microbial biomass measured as total lipid phosphate in soils of different organic content. Journal of Microbiological Methods 14 (3), 151–163. doi:10.1016/0167-7012(91)90018-l.

Gholizadeh, A., Neumann, C., Chabrillat, S., van Wesemael, B., Castaldi, F., Borůvka, L., et al., 2021. Soil organic carbon estimation using VNIR–SWIR spectroscopy: the effect of multiple sensors and scanning conditions. Soil and Tillage Research 211 105017 doi:10.1016/j.still.2021.105017.

Guerra, C.A., Bardgett, R.D., Caon, L., Crowther, T.W., Delgado-Baquerizo, M., Montanarella, L., Navarro, L.M., Orgiazzi, A., Singh, B.K., Tedersoo, L., Vargas-Rojas, R., Briones, M.J.I., Buscot, F., Cameron, E.K., Cesarz, S., Chatzinotas, A., Cowan, D.A., Djukic, I., van den Hoogen, J., Lehmann, A., Maestre, F.T., Marín, C., Reitz, T., Rillig, M.C., Smith, L.C., de Vries, F.T., Weigelt, A., Wall, D.H.,

Eisenhauer, N., 2021. Tracking, targeting, and conserving soil biodiversity. Science 371 (6526), 239–241. doi:10.1126/science.abd7926.

Guerra, C.A., Heintz-Buschart, A., Sikorski, J., Chatzinotas, A., Guerrero-Ramírez, N., Cesarz, S., Beaumelle, L., Rillig, M.C., Maestre, F.T., Delgado-Baquerizo, M., Buscot, F., Overmann, J., Patoine, G., Phillips, H.R.P., Winter, M., Wubet, T., Küsel, K., Bardgett, R.D., Cameron, E.K., Cowan, D., Grebenc, T., Marín, C., Orgiazzi, A., Singh, B.K., Wall, D.H., Eisenhauer, N., 2020. Blind spots in global soil biodiversity and ecosystem function research. Nature Communications 11 (1), 1–13. doi:10.1038/s41467-020-17688-2.

Halekoh, U., Højsgaard, S., 2014. A Kenward-Roger approximation and parametric bootstrap methods for tests in linear mixed models – the R package pbkrtest. Journal of Statistical Software 59 (9), 1–30. doi:10.18637/jss.v059.i09.

Heinze, S., Vohland, M., Joergensen, R.G., Ludwig, B., 2013. Usefulness of near-infrared spectroscopy for the prediction of chemical and biological soil properties in different long-term experiments. Journal of Plant Nutrition and Soil Science 176 (4), 520–528. doi:10.1002/jpln.201200483.

Hoerl, A.E., Kennard, R.W., 1970. Ridge regression: biased estimation for nonorthogonal problems. Technometrics 12 (1), 55–67. doi:10.1080/00401706.2000.10485983.

Hong, Y., Yu, L., Chen, Y., Liu, Y., Liu, Y., Liu, Y., Cheng, H., 2018. Prediction of soil organic matter by VIS–NIR spectroscopy using normalized soil moisture index as a proxy of soil moisture. Remote Sensing 10 (1), 28. doi:https://doi.org/10.3390/rs10010028.

Hunt, G.R., 1977. Spectral signatures of particulate minerals in the visible and near infrared. Geophysics 42 (3), 501–513. doi:10.1190/1.1440721.

Hutengs, C., Ludwig, B., Jung, A., Eisele, A., Vohland, M., 2018. Comparison of portable and benchtop spectrometers for mid-infrared diffuse reflectance measurements of soils. Sensors 18 (4), 993. doi:10.3390/s18040993.

Hutengs, C., Seidel, M., Oertel, F., Ludwig, B., Vohland, M., 2019. In situ and laboratory soil spectroscopy with portable visible-to-near-infrared and mid-infrared instruments for the assessment of organic carbon in soils. Geoderma 355, 113900. doi:10.1016/j.geoderma.2019.113900.

Izaurralde, R.C., Rice, C.W., Wielopolski, L., Ebinger, M.H., Reeves, J.B., Thomson, A.M., Harris, R., Francis, B., Mitra, S., Rappaport, A.G., Etchevers, J.D., Sayre, K.D., Govaerts, B., McCarty, G.W., 2013. Evaluation of Three Field-Based Methods for Quantifying Soil Carbon. PLoS ONE 8, 55560. doi:10.1371/journal.pone.0055560.

Jaconi, A., Poeplau, C., Ramirez-Lopez, L., Van Wesemael, B., Don, A., 2019. Log-ratio transformation is the key to determining soil organic carbon fractions with near-infrared spectroscopy. European Journal of Soil Science 70 (1), 127–139. doi:10.1111/ejss.12761.

James, G., Witten, D., Hastie, T., Tibshirani, R., 2013. An Introduction to Statistical Learning. Springer, New York, NY.

Janik, L.J., Soriano-Disla, J.M., Forrester, S.T., McLaughlin, M.J., 2016. Moisture effects on diffuse reflection infrared spectra of contrasting minerals and soils: a mechanistic interpretation. Vibrational Spectroscopy 86, 244–252. doi:10.1016/j.vibspec.2016.07.005.

Janik, L.J., Soriano-Disla, J.M., Forrester, S.T., 2020. Feasibility of handheld mid-infrared spectroscopy to predict particle size distribution: influence of soil field condition and utilization of existing spectral libraries. Soil Research 58 (6), 528–539. doi:doi.org/10.1071/sr20097.

Jansson, J.K., Hofmockel, K.S., 2020. Soil microbiomes and climate change. Nature Reviews Microbiology 18 (1), 35–46. doi:10.1038/s41579-019-0265-7.

Kerry, R., Rawlins, B.G., Oliver, M.A., Lacinska, A.M., 2009. Problems with determining the particle size distribution of chalk soil and some of their implications. Geoderma 152 (3–4), 324–337. doi:10.1016/j.geoderma.2009.06.018.

Knadel, M., Stenberg, B., Deng, F., Thomsen, A., Greve, M.H., 2013. Comparing predictive abilities of three visible-near infrared spectrophotometers for soil organic carbon and clay determination. Journal of Near Infrared Spectroscopy 21 (1), 67–80. doi:10.1255/jnirs.1035.

Knox, N.M., Grunwald, S., McDowell, M.L., Bruland, G.L., Myers, D.B., Harris, W.G., 2015. Modelling soil carbon fractions with visible near-infrared (VNIR) and mid-infrared (MIR) spectroscopy. Geoderma 239, 229–239. doi:10.1016/j.geoderma.2014.10.019.

Kreutziger, Y., Baade, J., Gleixner, G., Habekost, M., Hildebrandt, A., Schwichtenberg, G., et al., 2018. Collection of Data on Physical and Chemical Soil Properties in the Jena Experiment (Main Experiment). PANGAEA. doi:10.1594/PANGAEA.885439.

Kuang, B., Mouazen, A.M., 2011. Calibration of visible and near infrared spectroscopy for soil analysis at the field scale on three European farms. European Journal of Soil Science 62 (4), 629–636. doi:10.1111/j.1365-2389.2011.01358.x.

Kuang, B., Mahmood, H.S., Quraishi, M.Z., Hoogmoed, W.B., Mouazen, A.M., van Henten, E.J., 2012. Sensing soil properties in the laboratory, in situ, and on-line: a review. Advances in Agronomy 114, 155–223. doi:10.1016/b978-0-12-394275-3.00003-1.

Kusumo, B.H., Hedley, C.B., Hedley, M.J., Hueni, A., Tuohy, M.P., Arnold, G.C., 2008. The use of diffuse reflectance spectroscopy for in situ carbon and nitrogen analysis of pastoral soils. Soil Research 46 (7), 623–635. doi:doi.org/10.1071/sr08118.

Lange, M., Eisenhauer, N., Sierra, C.A., Bessler, H., Engels, C., Griffiths, R.I., Mellado-Vázquez, P.G., Malik, A.A., Roy, J., Scheu, S., Steinbeiss, S., Thomson, B.C., Trumbore, S.E., Gleixner, G., 2015. Plant diversity increases soil microbial activity and soil carbon storage. Nature Communications 6 (1), 1–8. doi:10.1038/ncomms7707.

Ludwig, B., Nitschke, R., Terhoeven-Urselmans, T., Michel, K., Flessa, H., 2008. Use of mid-infrared spectroscopy in the diffuse-reflectance mode for the prediction of the composition of organic matter in soil and litter. Journal of Plant Nutrition and Soil Science 171 (3), 384–391. doi:10.1002/jpln.200700022.

Ludwig, B., Sawallisch, A., Heinze, S., Joergensen, R.G., Vohland, M., 2015. Usefulness of middle infrared spectroscopy for an estimation of chemical and biological soil properties – underlying principles and comparison of different software packages. Soil Biology and Biochemistry 86, 116–125. doi:10.1016/j.soilbio.2015.03.015.

Lange, M., Habekost, M., Eisenhauer, N., Roscher, C., Bessler, H., Engels, C., Oelmann, Y., Scheu, S., Wilcke, W., Schulze, E.D., Gleixner, G., 2014. Biotic and abiotic properties mediating plant diversity effects on soil microbial communities in an experimental grassland. PLoS ONE 9 (5), e96182. doi:10.1371/journal.pone.0096182.

Ludwig, B., Linsler, D., Höper, H., Schmidt, H., Piepho, H.P., Vohland, M., 2016. Pitfalls in the use of middle-infrared spectroscopy: representativeness and ranking criteria for the estimation of soil properties. Geoderma 268, 165–175. doi:10.1016/j.geoderma.2016.01.010.

Marakkala Manage, L.P., Greve, M.H., Knadel, M., Moldrup, P., De Jonge, L.W., Katuwal, S., 2018. Visible-near-infrared spectroscopy prediction of soil characteristics as affected by soil-water content. Soil Science Society of America Journal 82 (6), 1333–1346. doi:10.2136/sssaj2018.01.0052.

Martínez-España, R., Bueno-Crespo, A., Soto, J., Janik, L.J., Soriano-Disla, J.M., 2019. Developing an intelligent system for the prediction of soil properties with a portable mid-infrared instrument. Biosystems Engineering 177, 101–108. doi:10.1016/j.biosystemseng.2018.09.013.

McBratney, A.B., Minasny, B., Viscarra Rossel, R.A., 2006. Spectral soil analysis and inference systems: a powerful combination for solving the soil data crisis. Geoderma 136 (1–2), 272–278. doi:10.1016/j.geoderma.2006.03.051.

Mellado-Vázquez, P.G., Lange, M., Bachmann, D., Gockele, A., Karlowsky, S., Milcu, A., Piel, C., Roscher, C., Roy, J., Gleixner, G., 2016. Plant diversity generates enhanced soil microbial access to recently photosynthesized carbon in the rhizosphere. Soil Biology and Biochemistry 94, 122–132. doi:10.1016/j.soilbio.2015.11.012.

Ng, W., Minasny, B., Montazerolghaem, M., Padarian, J., Ferguson, R., Bailey, S., McBratney, A.B., 2019. Convolutional neural network for simultaneous prediction of several soil properties using visible/near-infrared, mid-infrared, and their combined spectra. Geoderma 352, 251–267. doi:10.1016/j.geoderma.2019.06.016.

Nguyen, T.T., Janik, L.J., Raupach, M., 1991. Diffuse reflectance infrared Fourier transform (DRIFT) spectroscopy in soil studies. Soil Research 29 (1), 49–67. doi:10.1071/sr9910049.

Nocita, M., Stevens, A., Noon, C., van Wesemael, B., 2013. Prediction of soil organic carbon for different levels of soil moisture using Vis-NIR spectroscopy. Geoderma 199, 37–42. doi:10.1016/j.geoderma.2012.07.020.

Nocita, M., Stevens, A., Toth, G., Panagos, P., van Wesemael, B., Montanarella, L., 2014. Prediction of soil organic carbon content by diffuse reflectance spectroscopy using a local partial least square regression approach. Soil Biology and Biochemistry 68, 337–347. doi:10.1016/j.soilbio.2013.10.022.

Nocita, M., Stevens, A., van Wesemael, B., Aitkenhead, M., Bachmann, M., Barthès, B., Ben Dor, E., Brown, D.J., Clairotte, M., Csorba, A., Dardenne, P., Demattê, J.A.M., Genot, V., Guerrero, C., Knadel, M., Montanarella, L., Noon, C., Ramirez-Lopez, L., Robertson, J., Sakai, H., Soriano-Disla, J.M., Shepherd, K.D., Stenberg, B., Towett, E.K., Vargas, R., Wetterlind, J., 2015. Soil Spectroscopy: An Alternative to Wet Chemistry for Soil Monitoring. Advances in Agronomy 132, 139–159. doi:10.1016/bs.agron.2015.02.002.

Orgiazzi, A., Ballabio, C., Panagos, P., Jones, A., Fernández-Ugalde, O., 2018. LUCAS Soil, the largest expandable soil dataset for Europe: a review. European Journal of Soil Science 69 (1), 140–153. doi:10.1111/ejss.12499.

O'Rourke, S.M., Minasny, B., Holden, N.M., McBratney, A.B., 2016. Synergistic use of Vis-NIR, MIR, and XRF spectroscopy for the determination of soil geochemistry. Soil Science Society of America Journal 80 (4), 888–899. doi:10.2136/sssaj2015.10.0361.

Parikh, S.J., Goyne, K.W., Margenot, A.J., Mukome, F.N., Calderón, F.J., 2014. Soil chemical insights provided through vibrational spectroscopy. Advances in Agronomy 126, 1–148. doi:10.1016/b978-0-12-800132-5.00001-8.

R Core Team. R: A language and environment for statistical computing. R foundation for statistical computing. Vienna, Austria. https://www.R-project.org/, 2020.

Ramirez, K.S., Leff, J.W., Barberán, A., Bates, S.T., Betley, J., Crowther, T.W., Kelly, E.F., Oldfield, E.E., Shaw, E.A., Steenbock, C., Bradford, M.A., Wall, D.H., Fierer, N., 2014. Biogeographic patterns in below-ground diversity in New York City's Central Park are similar to those observed globally. Proceedings of the Royal Society B: Biological Sciences 281 (1795), 20141988. doi:10.1098/rspb.2014.1988.

Rasche, F., Marhan, S., Berner, D., Keil, D., Kandeler, E., Cadisch, G., 2013. midDRIFTS-based partial least square regression analysis allows predicting microbial biomass, enzyme activities and 16S rRNA gene abundance in soils of temperate grasslands. Soil Biology and Biochemistry 57, 504–512. doi:10.1016/j.soilbio.2012.09.030.

Reeves, J.B., 2010. Near-versus mid-infrared diffuse reflectance spectroscopy for soil analysis emphasizing carbon and laboratory versus on-site analysis: where are we and what needs to be done? Geoderma 158 (1–2), 3–14. doi:10.1016/j.geoderma.2009.04.005.

Reeves, J.B., McCarty, G.W., Hively, W.D., 2010. Mid- versus near-infrared spectroscopy for on-site analysis of soil. In: Viscarra Rossel, R.A., McBratney, A.B., Minasny, B. (Eds.), Proximal Soil Sensing. Springer, Dordrecht, pp. 133–142. doi:10.1007/978-90-481-8859-8_11.

Ricketts, M.P., Matamala, R., Jastrow, J.D., AntonopoulosRicketts, M.P., Matamala, R., Jastrow, J.D., Antonopoulos, D.A., Koval, J., Ping, C.L., Liang, C., Gonzalez-Meler, M.A., 2020. The effects of warming and soil chemistry on bacterial community structure in Arctic tundra soils. Soil Biology and Biochemistry 148, 107882. doi:10.1016/j.soilbio.2020.107882.

Rinnan, R., Rinnan, Å., 2007. Application of near infrared reflectance (NIR) and fluorescence spectroscopy to analysis of microbiological and chemical properties of arctic soil. Soil Biology and Biochemistry 39 (7), 1664–1673. doi:10.1016/j.soilbio.2007.01.022.

Rinnan, Å., Van Den Berg, F., Engelsen, S.B., 2009. Review of the most common pre-processing techniques for near-infrared spectra. TRAC Trends in Analytical Chemistry 28 (10), 1201–1222. doi:10.1016/j.trac.2009.07.007.

Roscher, C., Schumacher, J., Baade, J., Wilcke, W., Gleixner, G., Weisser, W.W., Schmid, B., Schulze, E.D., 2004. The role of biodiversity for element cycling and trophic interactions: an experimental approach in a grassland community. Basic and Applied Ecology 5 (2), 107–121. doi:10.1078/1439-1791-00216.

Seidel, M., Hutengs, C., Ludwig, B., Thiele-Bruhn, S., Vohland, M., 2019. Strategies for the efficient estimation of soil organic carbon at the field scale with vis-NIR spectroscopy: spectral libraries and spiking vs. local calibrations. Geoderma 354 113856 doi:10.1016/j.geoderma.2019.07.014.

Seybold, C.A., Ferguson, R., Wysocki, D., Bailey, S., Anderson, J., Nester, B., Schoeneberger, P., Wills, S., Libohova, Z., Hoover, D., Thomas, P., 2019. Application of Mid-Infrared Spectroscopy in Soil Survey. Soil Science Society of America Journal 83 (6), 1746–1759. doi:10.2136/sssaj2019.06.0205.

Soriano-Disla, J.M., Janik, L.J., Viscarra Rossel, R.A., Macdonald, L.M., McLaughlin, M.J., 2014. The performance of visible, near-, and mid-infrared reflectance spectroscopy for prediction of soil physical, chemical, and biological properties. Applied Spectroscopy Reviews 49 (2), 139–186. doi:10.1080/05704928.2013.811081.

Silvero, N.E.Q., Di Raimo, L.A.D.L., Pereira, G.S., Magalhãesde, L.P., Terrada, F.S., Dassan, M.A.A., Salazar, D.F.U., Demattê, J.A.M., 2020. Effects of water, organic matter, and iron forms in mid-IR spectra of soils: Assessments from laboratory to satellite-simulated data. Geoderma 375, 114480. doi:10.1016/j.geoderma.2020.114480.

Soriano-Disla, J.M., Janik, L.J., Allen, D.J., McLaughlin, M.J., 2017. Evaluation of the performance of portable visible-infrared instruments for the prediction of soil properties. Biosystems Engineering 161, 24–36. doi:10.1016/j.biosystemseng.2017.06.017.

Stenberg, B., 2010. Effects of soil sample pretreatments and standardized rewetting as interacted with sand classes on Vis-NIR predictions of clay and soil organic carbon. Geoderma 158 (1–2), 15–22. doi:10.1016/j.geoderma.2010.04.008.

Stenberg, B., Viscarra Rossel, R.A., Mouazen, A.M., Wetterlind, J., 2010. Visible and near infrared spectroscopy in soil science. Advances in Agronomy 107, 163–215. doi:10.1016/s0065-2113(10)07005-7.

A. Stevens, L. Ramirez-Lopez. An introduction to the prospectr package. R package Vignette. R package version 0.2.1. https://cran.r-project.org/web/packages/prospectr/vignettes/prospectr.html, 2020.

Stevens, A., Van Wesemael, B., Vandenschrick, G., Touré, S., Tychon, B., 2006. Detection of carbon stock change in agricultural soils using spectroscopic techniques. Soil Science Society of America Journal 70 (3), 844–850. doi:10.2136/sssaj2005.0025.

Stevens, A., Nocita, M., Tóth, G., Montanarella, L., van Wesemael, B., 2013. Prediction of soil organic carbon at the European scale by visible and near infrared reflectance spectroscopy. PloS One 8 (6) e66409 doi:10.1371/journal.pone.0066409.

Strecker, T., Macé, O.G., Scheu, S., Eisenhauer, N., 2016. Functional composition of plant communities determines the spatial and temporal stability of soil microbial properties in a long-term plant diversity experiment. Oikos 125 (12), 1743–1754. doi:10.1111/oik.03181.

Terhoeven-Urselmans, T., Schmidt, H., Joergensen, R.G., Ludwig, B., 2008. Usefulness of near-infrared spectroscopy to determine biological and chemical soil properties: importance of sample pretreatment. Soil Biology and Biochemistry 40 (5), 1178–1188. doi:10.1016/j.soilbio.2007.12.011.

Terra, F.S., Demattê, J.A., Viscarra Rossel, R.A., 2015. Spectral libraries for quantitative analyses of tropical Brazilian soils: comparing vis–NIR and mid-IR reflectance data. Geoderma 255, 81–93. doi:10.1016/j.geoderma.2015.04.017.

Terra, F.S., Viscarra Rossel, R.A., Demattê, J.A., 2019. Spectral fusion by Outer Product Analysis (OPA) to improve predictions of soil organic C. Geoderma 335, 35–46. doi:10.1016/j.geoderma.2018.08.005.

Viscarra Rossel, R.A., Walvoort, D.J.J., McBratney, A.B., Janik, L.J., Skjemstad, J.O., 2006. Visible, near infrared, mid infrared or combined diffuse reflectance spectroscopy for simultaneous assessment of various soil properties. Geoderma 131 (1–2), 59–75. doi:10.1016/j.geoderma.2005.03.007.

Viscarra Rossel, R.A., Adamchuk, V.I., Sudduth, K.A., McKenzie, N.J., Lobsey, C., 2011. Proximal soil sensing: an effective approach for soil measurements in space and time. Advances in Agronomy 113, 243–291. doi:10.1016/b978-0-12-386473-4.00005-1.

Vogel, A., Eisenhauer, N., Weigelt, A., Scherer-Lorenzen, M., 2013. Plant diversity does not buffer drought effects on early-stage litter mass loss rates and microbial properties. Global Change Biology 19 (9), 2795–2803. doi:10.1111/gcb.12225.

Vohland, M., Ludwig, M., Thiele-Bruhn, S., Ludwig, B., 2017. Quantification of soil properties with hyperspectral data: selecting spectral variables with different methods to improve accuracies and analyze prediction mechanisms. Remote Sensing 9 (11), 1103. doi:10.3390/rs9111103.

Wagner, D., Eisenhauer, N., Cesarz, S., 2015. Plant species richness does not attenuate responses of soil microbial and nematode communities to a flood event. Soil Biology and Biochemistry 89, 135–149. doi:10.1016/j.soilbio.2015.07.001.

Wehrens, R., 2011. Chemometrics with R: Multivariate Data Analysis in the Natural Sciences and Life Sciences. Springer, New York, NY.

Weisser, W.W., Roscher, C., Meyer, S.T., Ebeling, A., Luo, G., Allan, E., Beßler, H., Barnard, R.L., Buchmann, N., Buscot, F., Engels, C., Fischer, C., Fischer, M., Gessler, A., Gleixner, G., Halle, S., Hildebrandt, A., Hillebrand, H., de Kroon, H., Lange, M., Leimer, S., Le Roux, X., Milcu, A., Mommer, L., Niklaus, P.A., Oelmann, Y., Proulx, R., Roy, J., Scherber, C., Scherer-Lorenzen, M., Scheu, S., Tscharntke, T., Wachendorf, M., Wagg, C., Weigelt, A., Wilcke, W., Wirth, C., Schulze, E.D., Schmid, B., Eisenhauer, N., 2017. Biodiversity effects on ecosystem functioning in a 15-year grassland experiment: Patterns, mechanisms, and open questions. Basic and Applied Ecology 23, 1–73. doi:10.1016/j.baae.2017.06.002.

Wetterlind, J., Stenberg, B., 2010. Near-infrared spectroscopy for within-field soil characterization: small local calibrations compared with national libraries spiked with local samples. European Journal of Soil Science 61 (6), 823–843. doi:10.1111/j.1365-2389.2010.01283.x.

Willers, C., Jansen van Rensburg, P.J., Claassens, S., 2015. Phospholipid fatty acid profiling of microbial communities–a review of interpretations and recent applications. Journal of Applied Microbiology 119 (5), 1207–1218. doi:10.1111/jam.12902.

Wold, S., Sjöström, M., Eriksson, L., 2001. PLS-regression: a basic tool of chemometrics. Chemometrics and Intelligent Laboratory Systems 58 (2), 109–130. doi:10.1016/s0169-7439(01)00155-1.

Xia, Q., Rufty, T., Shi, W., 2020. Soil microbial diversity and composition: links to soil texture and associated properties. Soil Biology and Biochemistry 149 107953 doi:10.1016/j.soilbio.2020.107953.

Xu, D., Zhao, R., Li, S., Chen, S., Jiang, Q., Zhou, L., Shi, Z., 2019. Multi-sensor fusion for the determination of several soil properties in the Yangtze River Delta, China. European Journal of Soil Science 70 (1), 162–173. doi:10.1111/ejss.12729.

Xue, P.P., Carrillo, Y., Pino, V., Minasny, B., McBratney, A.B., 2018. Soil properties drive microbial community structure in a large scale transect in south eastern Australia. Scientific Reports 8 (1), 1–11. doi:10.1038/s41598-018-30005-8.

Yang, Y., Viscarra Rossel, R.A., Li, S., Bissett, A., Lee, J., Shi, Z., Behrens, T., Court, L., 2019. Soil bacterial abundance and diversity better explained and predicted with spectro-transfer functions. Soil Biology and Biochemistry 129, 29–38. doi:10.1016/j.soilbio.2018.11.005.

Zhang, Q., Wu, J., Yang, F., Lei, Y., Zhang, Q., Cheng, X., 2016. Alterations in soil microbial community composition and biomass following agricultural land use change. Scientific Reports 6 36587 doi:10.1038/srep36587.

Zornoza, R., Guerrero, C., Mataix-Solera, J., Scow, K.M., Arcenegui, V., Mataix-Beneyto, J., 2008. Near infrared spectroscopy for determination of various physical, chemical and biochemical properties in Mediterranean soils. Soil Biology and Biochemistry 40 (7), 1923–1930. doi:10.1016/j.soilbio.2008.04.003.

# Tables

**Table 1.** Summary statistics of soil physicochemical and PLFA-derived microbial properties[a] for the Jena Experiment site (n = 80).

| n = 80 | min | $Q_1$ | median | $Q_3$ | max | mean | SD |
|---|---|---|---|---|---|---|---|
| OC (g/kg) | 12.93 | 18.12 | 20.13 | 23.20 | 32.36 | 20.50 | 3.49 |
| N (g/kg) | 1.47 | 1.99 | 2.27 | 2.57 | 2.98 | 2.28 | 0.36 |
| IC (g/kg) | 5.48 | 7.96 | 12.45 | 19.65 | 39.90 | 16.57 | 10.78 |
| pH | 6.98 | 7.39 | 7.46 | 7.56 | 7.81 | 7.47 | 0.15 |
| C:N | 6.22 | 8.54 | 8.92 | 9.60 | 11.32 | 9.02 | 0.81 |
| Sand (%) | 3.10 | 8.10 | 14.95 | 33.75 | 47.50 | 20.36 | 13.58 |
| Clay (%) | 13.9 | 18.76 | 21.42 | 23.88 | 26.69 | 20.95 | 3.36 |
| $H_2O$ (%) | 13.50 | 15.34 | 16.23 | 18.01 | 20.18 | 16.56 | 1.65 |
| $PLFA_{TOT}$ (µg/g) | 14.05 | 21.10 | 24.65 | 27.85 | 37.38 | 24.32 | 4.71 |
| $PLFA_{MIC}$ (µg/g) | 6.69 | 9.95 | 11.43 | 13.11 | 17.02 | 11.45 | 2.26 |
| $PLFA_{BAC}$ (µg/g) | 5.81 | 8.38 | 9.61 | 10.86 | 14.68 | 9.61 | 1.84 |
| $PLFA_{FUN}$ (µg/g) | 0.85 | 1.44 | 1.83 | 2.19 | 3.14 | 1.84 | 0.51 |
| $PLFA_{G+}$ (µg/g) | 2.80 | 4.25 | 4.98 | 5.72 | 7.73 | 4.99 | 1.02 |
| $PLFA_{G-}$ (µg/g) | 0.35 | 0.63 | 0.76 | 0.90 | 1.36 | 0.77 | 0.21 |
| F:B | 0.13 | 0.16 | 0.19 | 0.21 | 0.31 | 0.19 | 0.035 |
| MIC:OC (‰) | 0.38 | 0.51 | 0.56 | 0.62 | 0.76 | 0.56 | 0.081 |
| G+:G− | 5.09 | 5.99 | 6.44 | 7.20 | 9.91 | 6.64 | 0.94 |

[a] F:B = ratio of fungal to bacterial PLFAs; MIC:OC = ratio of microbial PLFA biomass to organic carbon; G+:G− = ratio of gram-positive to gram-negative bacterial PLFAs.

**Table 2.** Validation results of VNIR and MIR PLSR calibrations of soil physicochemical properties for pre-treated and field-moist soil samples from the Jena Experiment site. Reported statistics are averages of 100 randomized calibration-validation runs. In each run, 40 soil samples were used for model calibration; validation statistics were calculated on the remaining 40 independent samples. RMSE column includes one standard deviation of the RMSE distribution in parentheses. VNIR/ MIR column gives validation statistics for the precision-weighted average of VNIR and MIR predictions.

| | | RMSE | $R^2$ | ME | RPD | RPIQ | RMSE | $R^2$ | ME | RPD | RPIQ | RMSE | $R^2$ | ME | RPD | RPIQ |
|---|---|---|---|---|---|---|---|---|---|---|---|---|---|---|---|---|
| | | VNIR | | | | | MIR | | | | | VNIR/MIR | | | | |
| dried/ground | OC (g/kg) | 1.483 (0.201) | 0.82 | −0.04 | 2.33 | 3.28 | 1.149 (0.235) | 0.88 | 0.07 | 2.91 | 4.01 | 1.033 (0.231) | 0.90 | 0.07 | 3.24 | 4.64 |
| | IC (g/kg) | 1.592 (0.161) | 0.98 | 0.12 | 6.77 | 7.73 | 0.854 (0.092) | 0.99 | 0.01 | 12.51 | 13.6 | 0.758 (0.083) | 0.99 | 0.01 | 14.15 | 16.31 |
| | N (g/kg) | 0.183 (0.022) | 0.73 | −0.01 | 1.92 | 2.96 | 0.143 (0.013) | 0.84 | 0.00 | 2.50 | 3.84 | 0.143 (0.015) | 0.84 | −0.01 | 2.46 | 3.79 |
| | Sand (%) | 4.48 (0.46) | 0.89 | −0.03 | 3.01 | 5.25 | 4.41 (0.44) | 0.89 | −0.01 | 3.06 | 5.30 | 4.09 (0.38) | 0.91 | −0.05 | 3.32 | 5.90 |
| | Clay (%) | 1.91 (0.22) | 0.67 | 0.02 | 1.77 | 2.57 | 1.87 (0.19) | 0.69 | −0.04 | 1.80 | 2.61 | 1.79 (0.19) | 0.72 | 0.02 | 1.86 | 2.73 |
| field-moist | OC (g/kg) | 2.244 (0.260) | 0.57 | −0.01 | 1.53 | 2.09 | 1.847 (0.246) | 0.72 | −0.03 | 1.83 | 2.56 | 1.777 (0.270) | 0.73 | 0.02 | 1.91 | 2.66 |
| | IC (g/kg) | 1.906 (0.259) | 0.97 | 0.03 | 5.55 | 6.48 | 1.263 (0.131) | 0.99 | −0.03 | 8.57 | 9.71 | 1.152 (0.150) | 0.99 | −0.02 | 9.38 | 10.93 |
| | N (g/kg) | 0.176 (0.021) | 0.75 | −0.01 | 2.02 | 3.08 | 0.159 (0.020) | 0.80 | 0.00 | 2.22 | 3.39 | 0.135 (0.014) | 0.85 | 0.00 | 2.58 | 3.99 |
| | Sand (%) | 4.67 (0.53) | 0.88 | −0.23 | 2.90 | 5.18 | 4.33 (0.41) | 0.90 | 0.02 | 3.16 | 5.48 | 3.93 (0.38) | 0.92 | −0.18 | 3.47 | 6.01 |
| | Clay (%) | 1.88 (0.18) | 0.68 | 0.00 | 1.78 | 2.58 | 1.83 (0.18) | 0.70 | −0.05 | 1.84 | 2.68 | 1.68 (0.16) | 0.76 | −0.03 | 2.06 | 2.97 |

**Table 3.** Validation results for VNIR and MIR PLSR calibrations of PLFA-derived soil microbial properties (µg/g) on pre-treated and field-moist soil samples from the Jena Experiment site. Reported statistics are averages of 100 randomized calibration-validation runs. In each run, 40 soil samples were used for model calibration; validation statistics were calculated on the remaining 40 independent samples. RMSE column includes one standard deviation of the RMSE distribution in parentheses. VNIR/MIR column gives validation statistics for the precision-weighted average of VNIR and MIR predictions.

| | | RMSE | $R^2$ | ME | RPD | RPIQ | RMSE | $R^2$ | ME | RPD | RPIQ | RMSE | $R^2$ | ME | RPD | RPIQ |
|---|---|---|---|---|---|---|---|---|---|---|---|---|---|---|---|---|
| | | VNIR | | | | | MIR | | | | | VNIR/MIR | | | | |
| dried/ground | $PLFA_{TOT}$ | 3.073 (0.312) | 0.56 | 0.00 | 1.51 | 2.10 | 2.763 (0.282) | 0.65 | −0.12 | 1.70 | 2.32 | 2.669 (0.273) | 0.68 | −0.09 | 1.77 | 2.40 |
| | $PLFA_{MIC}$ | 1.368 (0.126) | 0.62 | −0.03 | 1.62 | 2.17 | 1.244 (0.121) | 0.69 | −0.02 | 1.79 | 2.41 | 1.189 (0.108) | 0.72 | −0.02 | 1.90 | 2.55 |
| | $PLFA_{BAC}$ | 1.148 (0.106) | 0.59 | −0.02 | 1.57 | 2.03 | 1.072 (0.103) | 0.66 | −0.01 | 1.70 | 2.17 | 1.020 (0.089) | 0.68 | −0.01 | 1.78 | 2.27 |
| | $PLFA_{G+}$ | 0.653 (0.058) | 0.57 | −0.01 | 1.55 | 2.10 | 0.625 (0.060) | 0.62 | 0.01 | 1.61 | 2.15 | 0.582 (0.052) | 0.66 | 0.00 | 1.73 | 2.32 |
| | $PLFA_{G-}$ | 0.128 (0.016) | 0.61 | 0.00 | 1.63 | 2.08 | 0.116 (0.012) | 0.68 | −0.01 | 1.76 | 2.29 | 0.110 (0.011) | 0.71 | 0.00 | 1.87 | 2.51 |
| | $PLFA_{FUN}$ | 0.325 (0.033) | 0.59 | −0.01 | 1.57 | 2.23 | 0.292 (0.032) | 0.66 | −0.02 | 1.75 | 2.48 | 0.277 (0.029) | 0.70 | −0.02 | 1.83 | 2.60 |
| field-moist | $PLFA_{TOT}$ | 3.031 (0.298) | 0.57 | −0.05 | 1.53 | 2.07 | 3.238 (0.257) | 0.52 | −0.13 | 1.44 | 1.96 | 2.802 (0.228) | 0.64 | −0.10 | 1.66 | 2.29 |
| | $PLFA_{MIC}$ | 1.362 (0.141) | 0.62 | −0.03 | 1.61 | 2.20 | 1.539 (0.158) | 0.52 | −0.1 | 1.44 | 1.95 | 1.256 (0.126) | 0.68 | −0.04 | 1.77 | 2.37 |
| | $PLFA_{BAC}$ | 1.186 (0.116) | 0.57 | 0.00 | 1.52 | 1.96 | 1.301 (0.140) | 0.48 | −0.06 | 1.39 | 1.80 | 1.100 (0.113) | 0.63 | −0.02 | 1.65 | 2.12 |
| | $PLFA_{G+}$ | 0.705 (0.066) | 0.52 | −0.01 | 1.43 | 1.89 | 0.707 (0.074) | 0.50 | −0.01 | 1.40 | 1.90 | 0.637 (0.060) | 0.61 | −0.01 | 1.59 | 2.17 |
| | $PLFA_{G-}$ | 0.119 (0.013) | 0.66 | 0.00 | 1.71 | 2.18 | 0.148 (0.016) | 0.47 | −0.01 | 1.37 | 1.81 | 0.117 (0.014) | 0.67 | −0.01 | 1.75 | 2.27 |
| | $PLFA_{FUN}$ | 0.311 (0.032) | 0.62 | −0.02 | 1.62 | 2.29 | 0.328 (0.027) | 0.59 | −0.02 | 1.57 | 2.21 | 0.290 (0.025) | 0.67 | −0.02 | 1.75 | 2.46 |

**Table 4a.** Summary of linear mixed effects model analysis of plant treatment effects on OC, $PLFA_{BAC}$, $PLFA_{FUN}$ and F:B using laboratory-analytical data. General model structure: Y ~ SP + FG + SP × FG + (1|BLOCK)[a].

| | OC | | $PLFA_{BAC}$ | | $PLFA_{FUN}$ | | F:B | |
|---|---|---|---|---|---|---|---|---|
| **Random effects** | SD | | SD | | SD | | SD | |
| BLOCK | 1.94 | | 0.87 | | 0.32 | | 0.025 | |
| Residual | 2.47 | | 1.11 | | 0.27 | | 0.021 | |
| **Fixed effects** | Coefficient | 95%-CI | Coefficient | 95%-CI | Coefficient | 95%-CI | Coefficient | 95%-CI |
| Intercept | 17.92 | (15.17, 20.64) | 7.70 | (6.46, 8.92) | 1.40 | (0.97, 1.83) | 0.181 | (0.148, 0.214) |
| SP 2 | 1.68 | (-0.12, 3.48) | 1.12 | (0.31, 1.93) | 0.19 | (-0.01, 0.38) | 0.002 | (-0.014, 0.019) |
| SP 4 | 3.03 | (1.23, 4.83) | 2.34 | (1.53, 3.15) | 0.58 | (0.38, 0.77) | 0.028 | (0.010, 0.046) |
| SP 8 | 2.24 | (0.43, 4.03) | 2.02 | (1.21, 2.83) | 0.61 | (0.42, 0.81) | 0.037 | (0.020, 0.055) |
| SP 16 | 5.05 | (3.19, 6.91) | 3.26 | (2.42, 4.10) | 0.68 | (0.47, 0.88) | 0.023 | (0.004, 0.042) |
| FG 2 | – | – | – | – | – | – | -0.007 | (-0.020, 0.007) |
| FG 3 | – | – | – | – | – | – | -0.021 | (-0.038, -0.004) |
| FG 4 | – | – | – | – | – | – | -0.022 | (-0.039, -0.006) |

[a] SP = number of sown plant species; FG = number of plant functional groups; BLOCK = experimental treatment block. Intercept term corresponds to monocultures (SP and FG = 1). Dashes (–) indicate non-significant effects of the FG term; the SP × FG terms were not significant in any model and were excluded from the table.

**Table 4b.** Summary of linear mixed effects model analysis of plant treatment effects on OC, $PLFA_{BAC}$, $PLFA_{FUN}$ and F:B using VNIR/MIR estimates from field-moist soils. General model structure: Y ~ SP + FG + SP × FG + (1|BLOCK)[a].

| | OC | | $PLFA_{BAC}$ | | $PLFA_{FUN}$ | | F:B | |
|---|---|---|---|---|---|---|---|---|
| **Random effects** | SD | | SD | | SD | | SD | |
| BLOCK | 1.79 | | 0.76 | | 0.32 | | 0.025 | |
| Residual | 1.91 | | 0.85 | | 0.20 | | 0.008 | |
| **Fixed effects** | Coefficient | 95%-CI | Coefficient | 95%-CI | Coefficient | 95%-CI | Coefficient | 95%-CI |
| Intercept | 18.38 | (15.92, 20.83) | 8.47 | (7.42, 9.52) | 1.57 | (1.16, 1.99) | 0.185 | (0.153, 0.217) |
| SP 2 | 1.20 | (-0.19, 2.59) | 0.43 | (-0.19, 1.05) | 0.13 | (-0.02, 0.27) | 0.003 | (-0.003, 0.009) |
| SP 4 | 2.51 | (1.12, 3.89) | 1.40 | (0.78, 2.02) | 0.32 | (0.18, 0.47) | 0.001 | (-0.005, 0.008) |
| SP 8 | 2.16 | (0.77, 3.55) | 1.38 | (0.76, 2.00) | 0.31 | (0.16, 0.46) | 0.000 | (-0.006, 0.006) |
| SP 16 | 4.09 | (2.66, 5.52) | 2.25 | (1.61, 2.89) | 0.56 | (0.41, 0.71) | 0.008 | (0.001, 0.015) |
| FG 2 | – | – | – | – | – | – | 0.005 | (0.000, 0.010) |
| FG 3 | – | – | – | – | – | – | 0.009 | (0.003, 0.015) |
| FG 4 | – | – | – | – | – | – | 0.002 | (-0.004, 0.008) |

[a] SP = number of sown plant species; FG = number of plant functional groups; BLOCK = experimental treatment block. Intercept term corresponds to monocultures (SP and FG = 1). Dashes (–) indicate non-significant effects of the FG term; the SP × FG terms were not significant in any model and were excluded from the table.

**Table 5.** Estimation of PLFA-derived soil microbial properties (μg/g) with linear models of physicochemical bulk soil properties[a]. Average statistics of 100 randomized calibration-validation runs (RMSE standard deviations in parentheses). In each run, 40 soil samples were used for MLR model fitting; validation statistics were calculated on the remaining 40 independent samples.

| Soil property (Y) | RMSE | $R^2$ | ME | RPD | RPIQ |
|---|---|---|---|---|---|
| $PLFA_{TOT}$ | 3.37 (0.31) | 0.50 | -0.15 | 1.41 | 1.86 |
| $PLFA_{MIC}$ | 1.53 (0.13) | 0.55 | -0.02 | 1.48 | 1.99 |
| $PLFA_{BAC}$ | 1.27 (0.11) | 0.54 | -0.04 | 1.48 | 1.90 |
| $PLFA_{FUN}$ | 0.37 (0.03) | 0.50 | 0.00 | 1.42 | 1.99 |
| $PLFA_{G+}$ | 0.73 (0.06) | 0.49 | -0.02 | 1.41 | 1.88 |
| $PLFA_{G-}$ | 0.14 (0.01) | 0.55 | 0.00 | 1.49 | 1.93 |

[a] Linear model: Y ~ OC + N + IC + pH + $H_2O$ + Sand + Clay.

**Table 6.** Comparison of estimates of soil indicators for soil microbial community structure from VNIR/MIR spectroscopy and linear regression models of physicochemical bulk soil properties. Average statistics of 100 randomized calibration-validation runs (RMSE standard deviations in parentheses). In each run, 40 soil samples were used for model fitting; validation statistics were calculated on the remaining 40 independent samples.

| Soil property/model[a] | RMSE | $R^2$ | ME | RPD | RPIQ |
|---|---|---|---|---|---|
| MIC: OC | | | | | |
| VNIR/MIR (DG) | 0.060 (0.006) | 0.43 | -0.014 | 1.33 | 1.73 |
| VNIR/MIR (FM) | 0.071 (0.007) | 0.21 | -0.000 | 1.12 | 1.47 |
| Linear model | 0.072 (0.006) | 0.20 | 0.001 | 1.12 | 1.46 |
| F:B | | | | | |
| VNIR/MIR (DG) | 0.024 (0.002) | 0.52 | 0.000 | 1.44 | 2.20 |
| VNIR/MIR (FM) | 0.026 (0.002) | 0.43 | 0.001 | 1.31 | 1.97 |
| Linear model | 0.027 (0.003) | 0.42 | 0.000 | 1.31 | 1.89 |
| G+:G- | | | | | |
| VNIR/MIR (DG) | 0.78 (0.08) | 0.33 | 0.05 | 1.22 | 1.51 |
| VNIR/MIR (FM) | 0.83 (0.08) | 0.21 | 0.08 | 1.13 | 1.40 |
| Linear model | 0.87 (0.09) | 0.16 | -0.02 | 1.09 | 1.37 |

[a] F:B = ratio of fungal to bacterial PLFAs; MIC:OC = ratio of microbial PLFA biomass to organic carbon (‰); G+:G− = ratio of gram-positive to gram-negative bacterial PLFAs; DG = dried/ground soil; FM = field-moist soil. Linear model: Y ~ OC + N + IC + pH + $H_2O$ + Sand + Clay.

# Figures

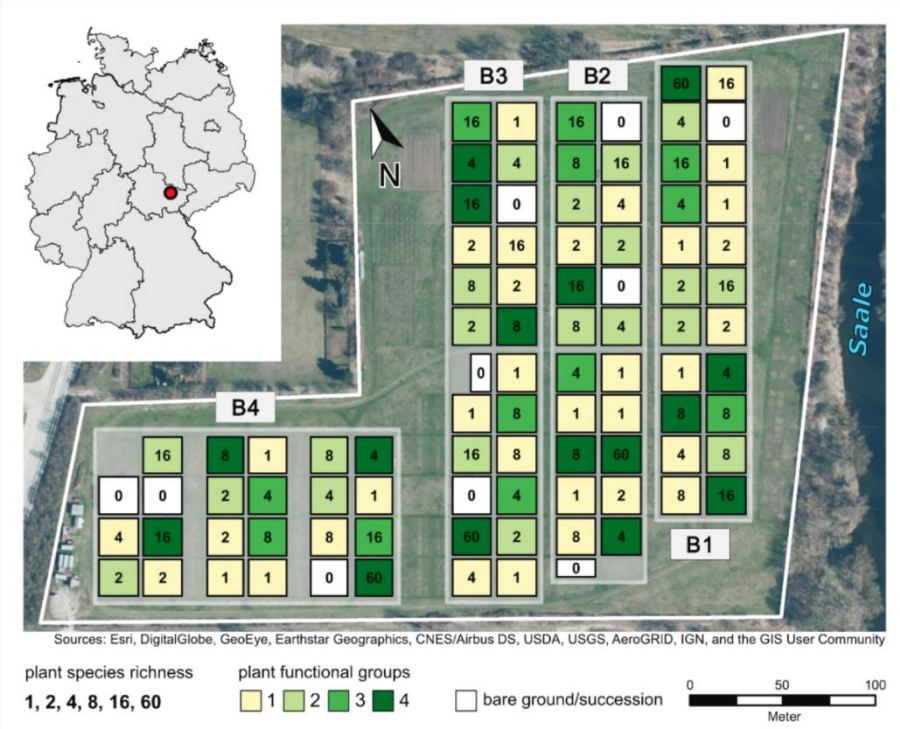


**Fig. 1.** Location and layout of the Jena Experiment field site. Experimental plots are arranged in four blocks parallel to the Saale river. Main experimental treatments replicated in each block are indicated, including plant species richness (number of sown and maintained plant species) and functional diversity (number of sown and maintained plant functional groups) (adapted from Strecker et al. (2016)).

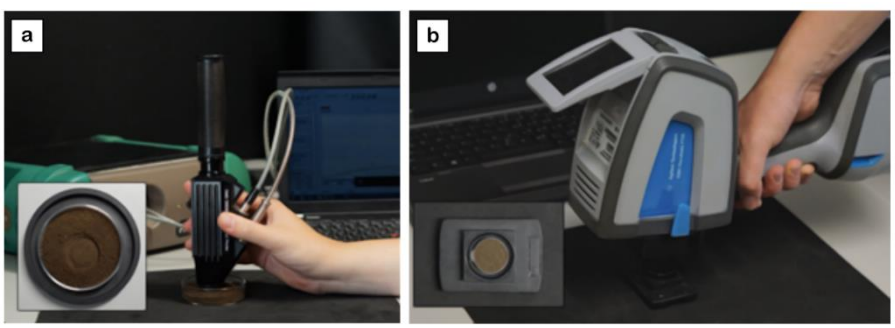


**Fig. 2.** Measurement of VNIR and MIR diffuse reflectance spectra on field-moist sample material with a) portable ASD FieldSpec 4 spectroradiometer with contact probe attachment and b) handheld Agilent 4300 FTIR instrument. Spectra were acquired with a measurement setup that facilitates potential on-site applications. The petri dish in a) has a diameter of d = 7 cm; the inset shows an example of the contact probe footprint (~3 $cm^2$). The filled sample holder in b) is 2 cm in diameter.

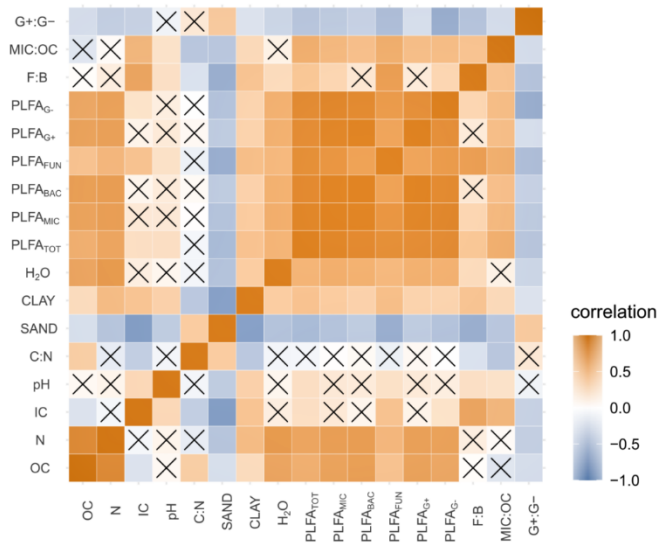


**Fig. 3.** Correlation matrix (*r*) of soil physicochemical and PLFA-derived microbial properties for the Jena Experiment site (n = 80). Non-significant ($p > 0.05$, pairwise t-test) correlations crossed out. F:B = ratio of fungal to bacterial PLFAs; MIC:OC = ratio of microbial PLFA biomass to organic carbon; G+:G− = ratio of gram-positive to gram-negative bacterial PLFAs.

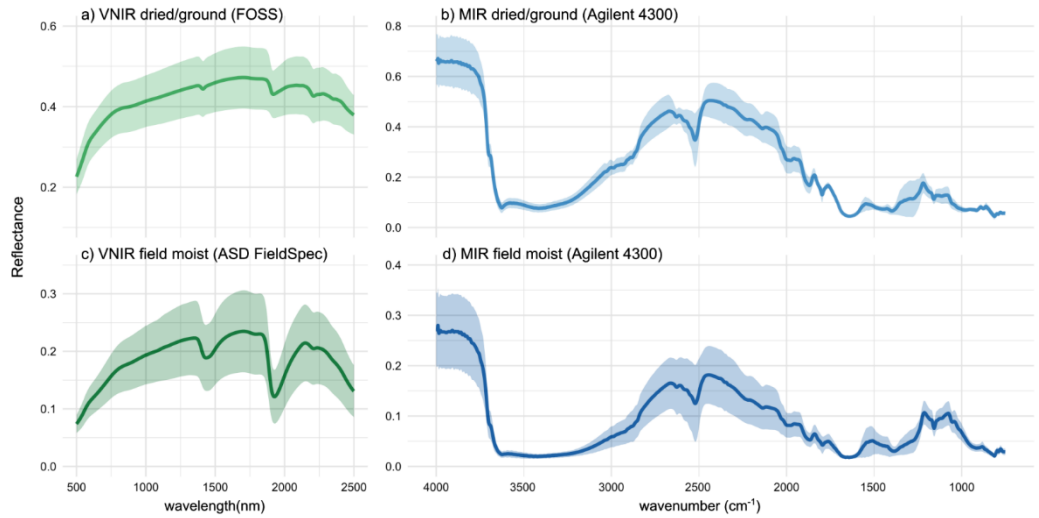


**Fig. 4.** VNIR and MIR reflectance spectra for dried/ground (a,b) and field-moist (c,d) soil samples. Solid curves represent the mean soil spectrum for each dataset; shaded bands represent ± two standard deviations from the mean spectrum. Note change of scale on the y-axis between subplots.

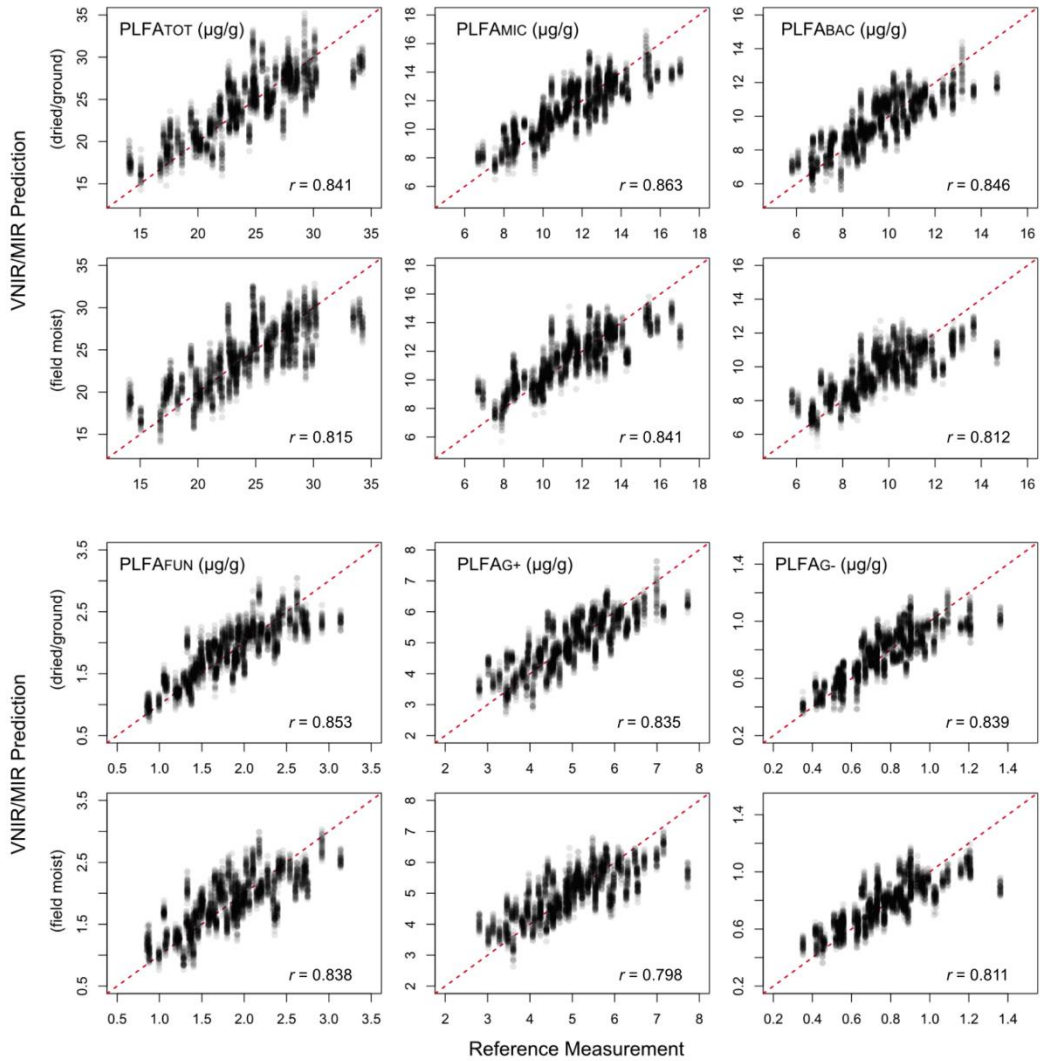


**Fig. 5.** Scatterplots of combined VNIR/MIR predictions for PLFA-derived soil microbial properties at the Jena site by soil pretreatment (dried/ground vs. field-moist). Model predictions were pooled over all independent validation samples across 100 randomized calibration-validation runs and plotted against the corresponding laboratory-analytical reference measurements.

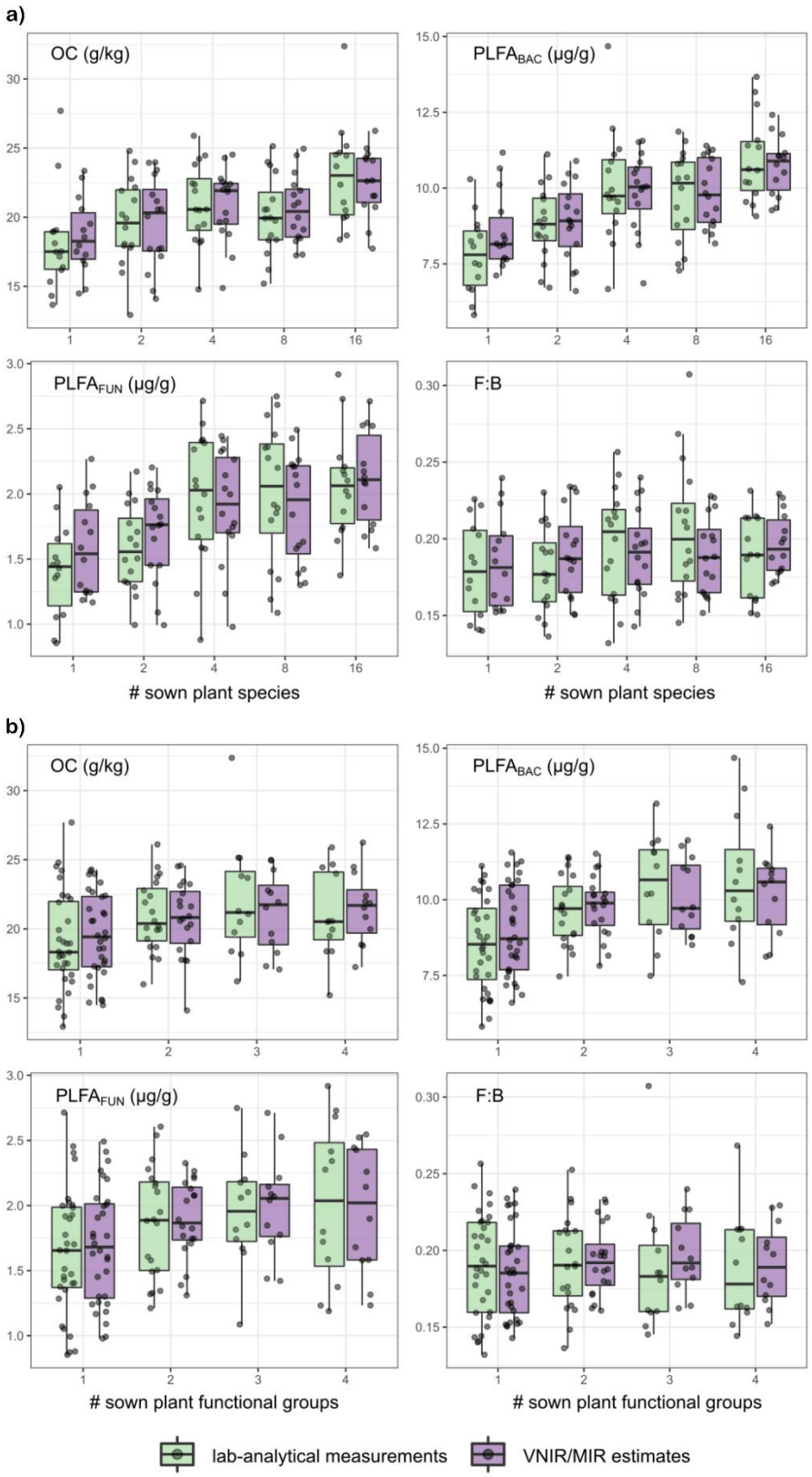


**Fig. 6.** Comparison of lab-analytical measurements and VNIR/MIR model estimates (from field-moist samples) for OC, PLFA$_{BAC}$, PLFA$_{FUN}$ and F:B at the main treatment levels: distributions by a) plant species richness and b) plant functional diversity.

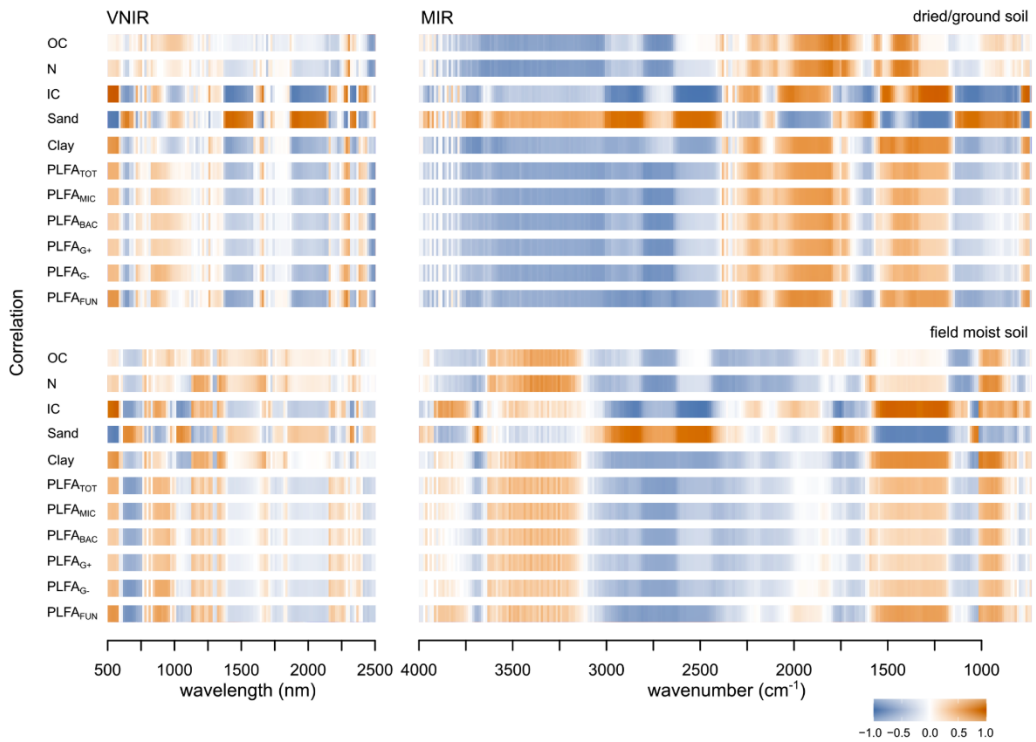


**Fig. 7.** Soil property correlation profiles for VNIR and MIR spectra (continuum-removed reflectance) collected on pre-treated (dried/ground) and field-moist soil samples showing linear correlations between individual spectral channels and soil physicochemical and microbial properties.

## Highlights

- VNIR/MIR allows accurate calibration of soil physicochemical properties.
- PLFA-derived microbial biomasses can be estimated with fair accuracy.
- PLFA estimates mediated by correlations with spectrally active soil constituents.
- Soil state (dry vs. field-moist) strongly impacts spectral correlation patterns.
- Soil spectroscopy could detect plant diversity effects on microbial biomasses